3-2022

Design Study for an Antenna Radar Cross Section Measurement Test Fixture

Wayne C. Kreimeyer

DESIGN STUDY FOR AN ANTENNA RADAR CROSS SECTION MEASUREMENT TEST FIXTURE

THESIS

Wayne C Kreimeyer, Captain, USAF

AFIT-ENG-MS-22-M-040

DEPARTMENT OF THE AIR FORCE
AIR UNIVERSITY

AIR FORCE INSTITUTE OF TECHNOLOGY

Wright-Patterson Air Force Base, Ohio

AFIT-ENG-MS-22-M-040

DESIGN STUDY FOR AN ANTENNA RADAR CROSS SECTION MEASUREMENT TEST FIXTURE

THESIS

Presented to the Faculty

Department of Electrical and Computer Engineering

Graduate School of Engineering and Management

Air Force Institute of Technology

Air University

Air Education and Training Command

in Partial Fulfillment of the Requirements for the

Degree of Master of Science in Electrical Engineering

Wayne C Kreimeyer, B.S.E.E.

Captain, USAF

March 24, 2022

AFIT-ENG-MS-22-M-040

DESIGN STUDY FOR AN ANTENNA RADAR CROSS SECTION MEASUREMENT TEST FIXTURE

THESIS

Wayne C Kreimeyer, B.S.E.E.
Captain, USAF

Committee Membership:

Michael D. Seal, Lt Col, Ph.D.,
Chair

Peter J. Collins, Ph.D.,
Member

Andrew J. Terzuoli, Ph.D.,
Member

AFIT-ENG-MS-22-M-040

Abstract

Stealth aircraft are designed to be undetected by radar by minimizing a return signature called the Radar Cross-Section (RCS). Therefore, it is essential to understand how antennas, which are necessary for communication, affect the overall RCS of the aircraft, so that their effects can be managed. Antenna RCS is commonly measured in a compact range, at a component level. So, the antenna needs a structure to support it, also referred to as a test fixture, that does not interfere with the measurement process. This thesis seeks to minimize the RCS of a test fixture, over a particular frequency band, while meeting other geometric constraints by evaluating different geometries. The result of this thesis is a test fixture design that has a low RCS which is separable from the signature of the antenna under measurement, while providing an appropriate near field environment for the antenna.

Table of Contents

Page

List of Figures

Figure Page

List of Tables

Table Page

DESIGN STUDY FOR AN ANTENNA RADAR CROSS SECTION MEASUREMENT TEST FIXTURE

I. Introduction

1.1 Problem Background

The purpose of stealth aircraft or Low Observable (LO) aircraft is to increase survivability in contested environments by breaking the kill chain. The kill chain is the entire process required to successfully engage an aircraft, and the steps of the kill chain include: find, fix, track, target, engage, and assess. If any of the first five step can be interrupted, then the kill chain has been broken and the aircraft is likely to survive a given engagement. The primary way by which LO aircraft break the kill chain, across the find, fix, and track phases is commonly referred to as signature based survivability.

Signature based survivability requires knowledge of the complete signature for a system so that both the design and tactical employment can be managed [2]. This requires knowledge of the complete signatures for the overall combat system including its mission systems, most specifically antennas which have two generally competing electromagnetic requirements. First, antennas must be able to radiate, and secondly antennas can't overly degrade the signature suppression of the system, which requires knowledge of the antenna Radar Cross-Section (RCS) [3]. Typical antenna measurement fixtures are designed for testing the radiating performance of the antenna [4] . However, extracting the scattering performance require a different test fixture that is compatible with low RCS measurements. This uncommon requirement leads to the need to design, at the unclassified level, basic fixtures that are amenable to making the necessary scattering measurements.

1.2 Current Problem

The constraints that this fixture must address are linked to the different sources of scattering from an antenna which are structural, antenna-mode and grating lobes. The most significant for the test fixture design is the antenna modal component. The near field of an antenna affects radiation efficiency because it can shift the modalities of the antenna resonance. So, the test fixture for RCS antenna has to provide a near-field environment that is similar to what the as-employed environment will be, so that the antennas resonance isn't changed significantly by the test fixture. Likewise, the test fixture has to be sufficiently similar to the employed environment so that the structural implications, like the cavity that the aperture the antenna is in, or it's coupling to a surface and the actual physical shaping of the antenna is oriented correctly and not obscured by the fixture [3]. In addition to these requirements, the fixture itself must minimize unintended surface waves reengaging with the antenna in a manner that is dissimilar to the of the installed environment, as this will significantly perturb the measurements. Finally, the fixture has to have a RCS signature that is lower than the object that is being measure in the angular range of interest or if not low enough, then at least cleanly separable from the antenna RCS that is being measured [5]. Thus, there are a great many constraints on this type of test fixture because of what specific nature of the intended measurement.

1.3 Test Fixture Requirements

The requirements for the antenna test fixture developed in this thesis are as follows. The fixture must fit in the quiet zone (20 ft wide X 25 ft long X 20 ft high) of a specific compact range. The fixture will have a flat top, housing the device under test, and be designed to operate in a 500 MHz to 2 GHz frequency range. Extending the usable frequency range as broadly as possible from 100 MHz to 18 GHz is desirable but not a requirement. The area of the Device Under Test (DUT) area is required to be a diamond 42 inches in length and 24 inches in depth. The azimuth observation angle requirement for low monostatic RCS measurements is +/-70 degree from the fixture reference or nose. The elevation look angle requirement for low monostatic RCS is -5° to +40° below and above the waterline. The distance from the test fixture edge to the DUT edge is required to be 5 wavelengths at all, or sub-threshold to most, operating frequencies. The bottom surface of the test fixture curvature is required to be 2nd derivative continuous, while the upper flat area profile is open for consideration. However, for a radius and straight shaped profile, the transition point from line to curve is required to occur in advance of the DUT area's forward edge ($>$ 30 inches from the center of the DUT area). Finally, the design must be manufacturable, which will inform design complexity considerations. These requirements are graphically presented in Figure 1 and Figure 2, and tabulated in Table 1.

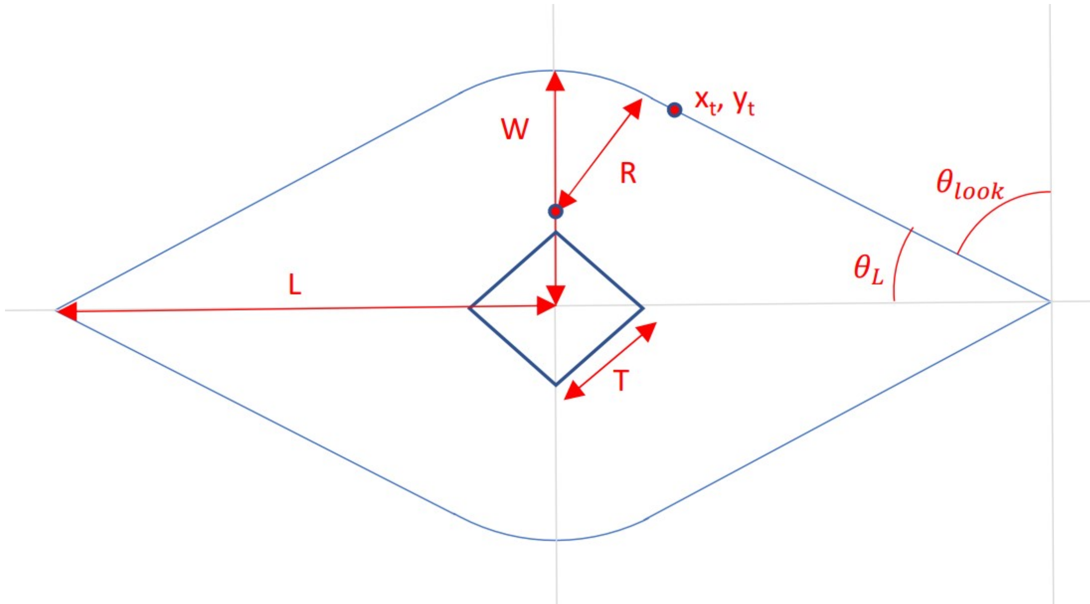

Figure 1: Top view of notional test fixture diagram with variables. L is the length form the the origin to the tip. W is width from the origin to the side. R is the radius from the Y-axis to the width. T is the DUT edge length. x_t, y_t is the transition point from the straight line to the curve. θ_{look} is the angle when looking at the point. θ_L is the internal half angle.

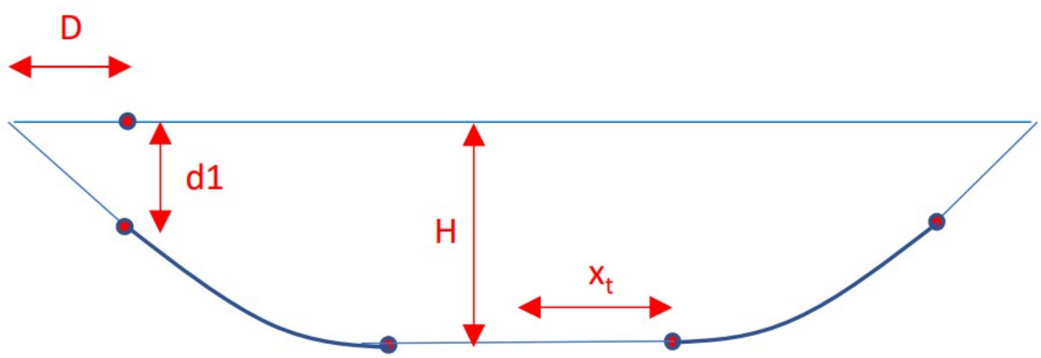

Figure 2: Side view of notional test fixture diagram with variables. H is the height of the test fixture. D in the inset and d1 is the depth of the straight angle before the curve, so the design is manufacturable. x_t is the same as the x_t in Figure 1 for the transition point but is the length of the radius for the flat bottom circle.

Table 1: Summary of requirements for the antenna test figure

Requirements	Desired Specifications
Size	25 ft (length) x 20 ft (wide) x 20 ft (height)
Test fixture design	Flat top
Device under Test (DUT) area	Diamond shape with 42 inches in length and 24 inches deep
Frequency Range	Threshold 500 MHz to 2 GHz Objective 100 MHz to 18 GHz
Azimuth look angle	$\pm 70°$
Elevation look angle	$-5°$ to $+40°$
Distance for the test fixture edge to DUT edge	5 wavelengths (5λ)
The bottom surface of the test fixture	2^{nd} derivative continues
For line-fillet shape, the transition point from line to the curve	before the DUT area (> 30inches from the center of the DUT area)
Design	Can be manufactured

1.4 Research Objectives

The research evaluates several aspects of the physical test fixture design to reduce risks and establish or document the applicability of certain practices. However, it is purely a body geometry based process, and therefore cannot represent the best achievable performance. The fixture design requirements themselves exhibit numerous and competing geometric constraints, which must be addressed. Therefore, the primary methods of this study are the application of CEM methods, leading to recommendation for perfectly conducting physical design dimensions. Multiple types of CEM prediction methods are used to address different aspects of the design requirements in a sequential manner, which may be taken as a foundation for more refined design work. Finally, simulations incorporating all the developed design decision recommendations are executed and evaluated to quantify the expected design performance.

1.5 Document Overview

The document is organized into four primary chapters, with supporting short chapters and sections. The literature review components are provided in-line as the sections progress. Otherwise, the chapters flow from background and theory through specific problem development and design requirements: Chapter II Background and Theory, Chapter III Specific Problem Development and Design Requirements, Chapter IV Geometric Optics (GO) and Geometry Based Design Refinement, Chapter V Test Surface Method of Moments (MoM)s Based Design Refinement, Chapter VI Overall 3-D Surface MoMs Based Design Refinement, Chapter VII (Conclusion).

Chapter II (Background and Theory) discusses the RCS of antennas and their importance, and the duality of radiation efficiency versus scattering efficiency, both in- and out-of-band. This chapter also discusses Computational Electromagnetics (CEM) model types that are used throughout the work, including GO, Geometrical Theory of Diffraction (GTD) and MoM. The lower computational cost methods are specifically highlighted, as early conclusions are drawn from them regarding planform alignment based performance bounds, specific to this test fixture.

Chapter III (Specific Problem Development and Design Requirements) discusses the requirements of the project and the identification of specific limitations. This chapter establishes the electrical size domain of the test fixture and the utility of GO based methods for basic shape design at the given frequencies, followed by some low level analysis.

Chapter IV (GO and Geometry Based Design Refinement) describes and discusses GO based angle constraints developed for a basic planform down-select between two profiles. A comparison is made between a radius straight design versus a second derivative continuous design, although the selection is not finalized until the next chapter. Additionally, some bounds on the overall geometry by nose angle and device under test to edge distance are established, which further limit the performance of the potential designs.

Chapter V (Test Surface MoMs Based Design Refinement) describes and discusses a process of selecting the frequencies and geometries for which RCS values will be evaluated and brings the geometry form down-selection to completion. A five point response surface of geometry values is established through analytic means and the RCS results calculted via the MoM on upper surface geometries. The nose sector data PCUM results are tabulated across frequencies for comparison with geometry based device under test stand-off distances decay metrics to arrive at a recommended upper surface geometric profile.

Chapter VI (Overall 3-D Surface MoMs Based Design Refinement) describes and discusses the 'boat hull' shape definition, completing the 3D geometry selection process. The requirements for accurate MoM based calculations discussed as well as methods of implementing the tested geometry and mesh. Specifically, the mesh requirements are documented, as well as the scripted geometry build methods. The method of determining the angular resolution for the RCS calculations is also described. Finally, the RCS data production process is documented, exemplar plots of angular RCS data are presented, and PCUM 50 and PCUM 90 statistics data over frequencies of interest are tabulated to support the complete data production package.

Chapter VII (Conclusion) states the final research outcomes, itemizes contributions and proposes follow-on efforts for future research.

II. Background and Literature Review

This section will cover the background of the Radar Cross-Section (RCS) antenna. Then, Computational Electromagnetics (CEM) will be covered with the geometric optic models and the geometric theory of diffraction to get a quick asymptotic for a rough design. Then Method of Moments (MoM) will be used to get an exact solution because the test fixture will be a perfect electric conductor (PEC) body. Then cover the importance of planform boundaries in reducing the RCS.

2.1 RCS of antennas background

Antennas have a requirement to receive and radiate electromagnetic energy, and of these requirements dictates the aperture size to achieve that radiation pattern [6]. Therefore, antennas are particularly challenging to design for low RCS.

Nonetheless, antennas continue to be designed and tested for both radiation efficiency and low RCS like the microstrip antenna using a uniplanar compact electromagnetic bandgap [7], or a patch array antennas using a method based on electromagnetic bandgap absorber by using a conducting polymer [8].

2.2 Background of CEM model types

There are multiple model types to address different requirements in terms of electrical size and computational time. Generally asymptotically, techniques like Geometric Optics (GO) and Geometrical Theory of Diffraction (GTD) methods are going to be much faster than an exact methods like the MoM. GO method are used to test the the initial geometry and concepts, which are later modeled via the MoM [9]. The GTD is employed for initial edge scattering estimates initial wave interactions with the edges.The well known, Uniform Theory of Diffraction (UTD) methods are not needed for this case because of mono-static radar case does not create shadow boundaries crossings. Calculating traveling waves interactions with the edges requires the MoM. MoM is needed because the requirement is to reduce the surface currents in the Device Under Test (DUT) area and asymptotic methods do not model this phenomenon.

2.3 Planform Alignment based bounds on RCS

Planform is when multiple edges have the same angle as each other or another was to think about it is the edges are parallel to each other. The iconic example of this is to B-2 bomber where all the edges are parallel to the two leading edges of the plane. This allows for spike herding or directing the energy in a known direction which can then be worked around. However, this is most effective in the optical regime, noted in Figure 3. The planform bounds or structural shape is the most effect and direct way in realizing low RCS returns. Radar Absorbing Material (RAM) is a supplement to stealth shape[10]. So, the primary emphasis must be placed on planform bounds. The planform bounds or shape direct waves being scattered away for radar receiver [11].

III. Specific Problem Development and Design Requirements

3.1 Preamble

This section presents an evaluation and analysis of the given requirements and points out several constraints and the needed adjustments to arrive at a workable set requirements. The initial analysis is purely geometrical. The second phase of analysis validates that the electrical size of the test fixture at the lowest frequency, or longest wavelength, lies is in the optical scattering region. This enables certain angular constraints to be assessed without resorting to exact solution methods through the application of analytic Radar Cross-Section (RCS) estimates, based on physical optics methods.

3.2 Identification

The requirements list in section 1.3 and Table 1 define an idealized test fixture that is impossible to realize. The problem is over-constrained. First, the set the requirements that are not negotiable are:

1. Fit inside the quiet zone (20 ft wide X 25 ft long X 20 ft High)
2. The top surface is flat, to which the Device Under Test (DUT) is mounted
3. Minimum frequencies range: 500 MHz to 2 GHz
4. The device under test (DUT) area is a Diamond with 42 inches in length and 24 inches deep.
5. The bottom surface of test fixture curvature is 2nd derivative continues

6. For radius and straight shape, the transition point from line to a curve is before the DUT area ($>$ 30 inches from the center of the DUT area)

7. The design must be manufacturable, although this is generally assessed only in the shape complexity

The remaining requirements provide the negotiable trade space for arriving at a satisfactory test fixture. These include the azimuth look angle constraints, the distance from the DUT to the body edge, etc. list to set up the next several paragraphs.

The Azimuth look angle of $\pm 70°$ directly competes with distance from the test fixture edge to the DUT edge requirement for five wavelengths (5λ) of setback, while retaining text fixture dimensions inside the proposed compact range quiet zone. To keep the largest distance possible from the test fixture edge to DUT edge, the Azimuth look angle is reduced to $\pm 45°$, and the depth of the fixture from 24 inches to 30 inches creating space to install an optional rotating mount for the DUT area. In this manner, the lesser working angle is partially compensated for by rapid DUT re-orientation. However, it does increase fabrication and measurement complexity.

The requirement for a distance from the test fixture edge to the DUT edge of 5λ is best expressed in literal dimensions. As always, wavelength is base on the frequency as shown in equation Equation (1).

$$\lambda = \frac{c}{f} \tag{1}$$

λ is the wavelength which equals the c (the speed of light in m/s) divided by f (Frequency in Hz or 1/s). The largest distance allowable is based on the limitation of the quiet zone that places the test fixture's edge at 10ft from the center, then subtracting the distance of the DUT zone from the center, which is just under 2.5 ft. This gives a distance of 7.5 ft (2.286 meters), which makes the lowest frequency for which the 5λ setback is possible 656 MHz. At 500 MHz at the max distance of 7.5 ft yields only 3.81 wavelengths of setback. Because of the physical limitations of the quiet zone, achieving 5λ at 500 MHz is impossible. However, an impetus remains to maximize the distance during design, in partial fulfillment of the requirements. Conversely, the elevation look angle requirement for -5° to +40° from waterline may be used without modification during the design process. The requirement changes discussed thus far, are itemized in Table 2.

Table 2: Updated summary of requirements for the antenna test figure after evaluating requirements that are not negotiable and the requirements that were adjusted.

Requirements	Desired Specifications	Updated
Size	25 ft (length) x 20 ft (wide) x 20 ft (Height)	No Change
Test fixture design	Flat top	No Change
Target under Test (TUT) area	a Diamond with 42 inches in length and 24 inches deep	a Diamond with 42 inches in length and 30 inches deep
Frequency Range	Threshold 500 MHz to 2 GHz Objective 100 MHz to 18 GHz	No Change
Azimuth look angle	$\pm 70°$	$\pm 45°$
Elevation look angle	$-5°$ to $+40°$	No Change
Distance for the test fixture edge to TUT edge	5 wavelengths (5λ)	Maxims when designing
The bottom surface of the test fixture	2nd derivative continues	No Change
For line-fillet shape, the transition point from line to the curve	before the TUT area (> 30inches from the center of the TUT area)	No Change
Design	Can be manufactured	No Change

3.3 Geometric Optics Validation

With the over constrained requirements relaxed or changed, it remains to otherwise maximize performance, across the remaining requirements. If the a scatterer's electrical size falls into the optical region, then quick and accurate analysis can be done with Geometric Optics (GO) based RCS methods to find the specular edge angles needed to avoid placing the main lobe into the nose or measurement sector. It is further possible to to test this requirement against the maximize edge to DUT distance. The lowest frequency of 500MHz, where the wavelength is 0.6 meters or 1.97 feet bounds the analysis. To be in Optical Region the circumference of the scatterer must be 10 wavelengths or greater,

$$10 \leq \frac{2\pi a}{\lambda} \tag{2}$$

where, 'a', is the radius of the sphere bounding the scatterer. To be 10 waves or greater then requires a $\geq$ 3.135 ft (Figure 3) which is just larger than fixture dimensions. When a = 7 ft the circumference per wavelength is 22.3. So, GO can be used to determine where the lobes appear at 500MHz at different angles. The lobe width is based on the electrical size, which may be simply view as the number of wavelengths that will fit on the fixture edge at a given frequency. Smaller electrical size objects have wider lobes, so the worst case should be selected. The length of eight feet was selected such that the max length for the adjacent length would be 10.0 feet, Length minus x_t (12.5 -2.5) and the angle are therefore less than 45 degree.

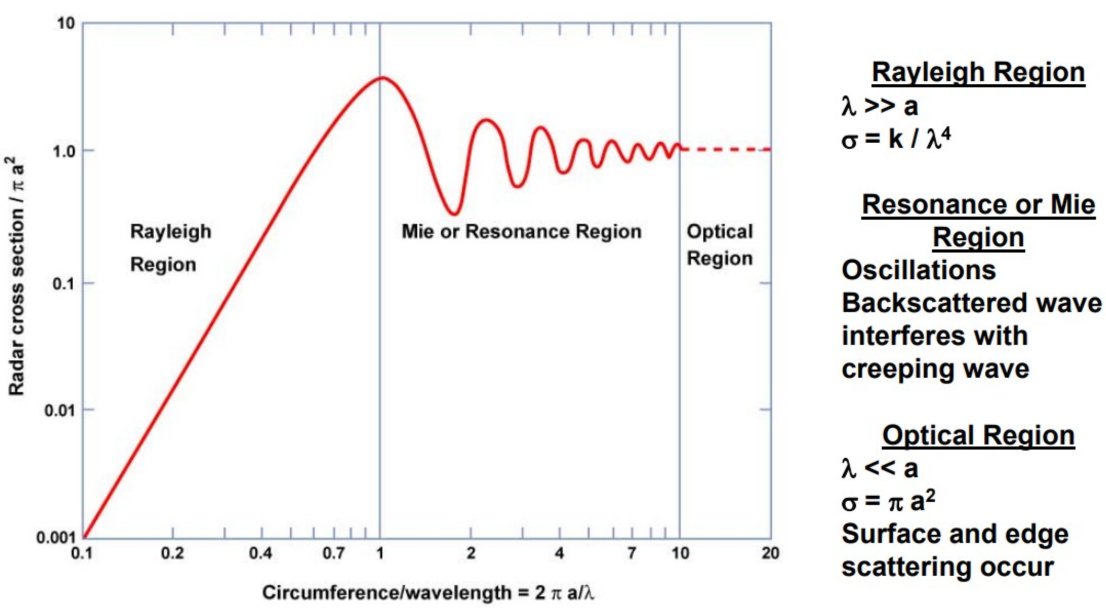

Figure 3: RCS of perfect electric conductor (PEC) Sphere [1]

GO can be used because even using a small width of 7 ft, 'a' in eq. (2) is double of what is need to be in the optical region, and geometry has only a few distinct scattering features.Presumably, the tip scattering will be dominated by the long edges, continuous and 2nd derivative continuous curves.

3.4 θ_{look} Angle Analysis

With the test fixture in the optical scattering region the next step is to use GO to determine what θ_{look} angle is needed to avoid placing the primary spectral lobes in the observation angle zone. The Hip Pocket RCS calculations by Air Force Institute of Technology (AFIT) Low Observables, Radar, and Electromagnetics (LORE) Processing Integrated Environment (ALPINE) were used to analyze where the lobes would manifest based on different angles. To overcome the limitation of program and highlight the 45°, 135°, 225° and 315° angles, fiducial spikes were added at each of thees angles. This helps identify lobe positions with respect to the -45° to 45° azimuth look angle.

To avoid the main lobe occupying the +/-45° angle, the wedge angle must be 38° or the angle from the point must be 52°, as shown in Figure 4, which limits the width of the fixture to 9.76 ft. The angle required to avoid the first side lobe was 32° or the angle from the point being 58° as shown in Figure 5, which further limits the width to 7.81 ft. The removal of the secondary lobe will limit the width greatly for the 5λ requirement, so the design was only specified to avoid the main lobe effect.

Although unreliable, 100MHz, Figure 6, and 200MHz, Figure 7, cases were also investigated to estimate whether these lower frequency values could be considered in the angle specification. However, even discounting the validity uncertainty, the main lobes were to wide for consideration in the design.

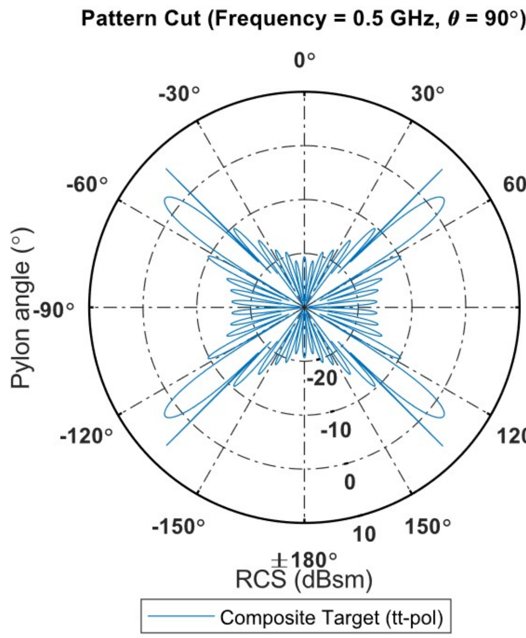

Figure 4: $\theta_{look} = 52°$ angle with 45° spikes. The main lobe at 500MHz is outside the -45° thru 45° measurement zone. The width is limited to 9.76 ft.

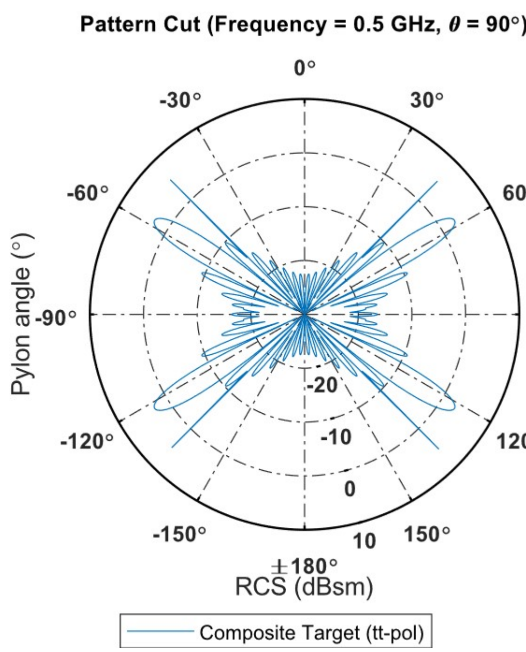

Figure 5: $\theta_{look} = 58°$ angle with 45° spikes, The first side lobe at 500MHz is outside the -45° thru 45° measurement zone. The width is limited to 7.81 ft.

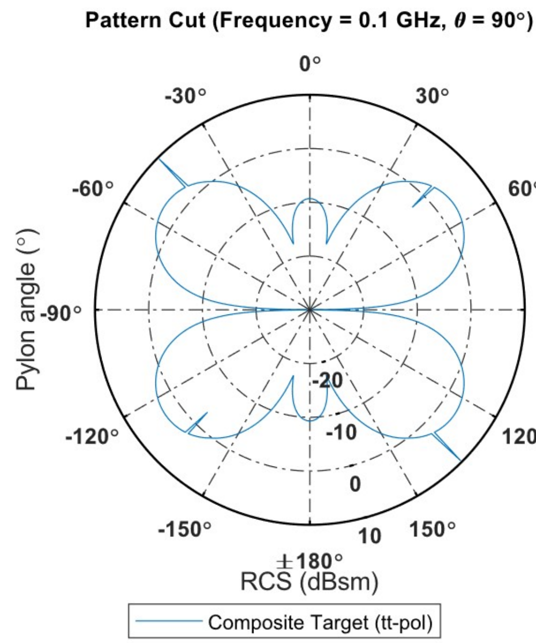

Figure 6: $\theta_{look} = 52°$ angle with 45° spikes, The main lobe at 100MHz is inside the -45° thru 45° measurement zone and main lobe is too wide for design angle consideration.

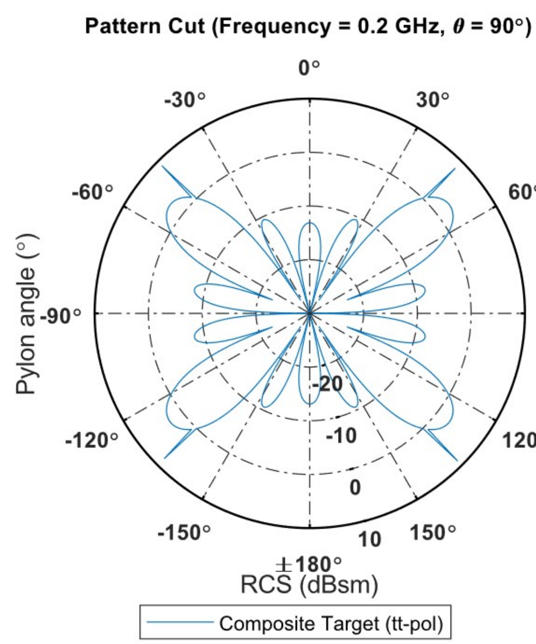

Figure 7: $\theta_{look} = 52°$ angle with 45° spikes, The main lobe at 200MHz is inside the -45° thru 45° measurement zone and main lobe is too wide for design angle consideration.

The angle that avoids the main lobe while providing the largest fixture width, and therefore the DUT to edge setback distance is $\theta_{look} = 52°$ or $\theta_L = 38°$ according to this analysis method.

3.5 Postamble

The design requirements were adjusted to remove the over restraints. For the adjusted requirements, the test fixture was shown to be large enough to use GO based methods for analysis on frequencies from 500MHz to 2GHz. Both GO and hip pocket RCS methods were used to determine a $\theta_{look} \geq 52°$ or $\theta_L \leq 38°$ requirement which avoids the main scattering lobes entering the nose or measurement region. This in turn sets constraints on the length and width of the fixture, inside the bounding quiet zone size restriction. The results are used in the following section.

IV. GO and Geometry Based Design Refinement

4.1 Preamble

This section addresses the requirements to find, intermediate geometric variables including, x_t and the internal angle θ_L within the design specifications with respect to the input variables L is for Length, W is for width, and R is for radius length, as shown in Figure 1. The first step is to find and analyze the combinations of L, W, & R that meet the $x_t \geq 3.0$ feet requirement, with a 0.5 foot margin from the Device Under Test (DUT). Next, the angular constraint theta, is addressed which comes directly from $\theta_L \leq 38°$ because $\theta_{look} \geq 52°$ as shown in Figure 4. In this section, only two different primary axis lengths, L, are evaluated. One is the full size of the quiet zone of 25 foot which makes L = 12.5 ft and the other is a reduced profile, 20% smaller at L = 10 ft. These results define the parameters for a radius-straight profile.

These dimensions are used as a in the cubic spline formula to create the alternative spline/second derivative continuous shape.

4.2 GO Based Angle Constraint developed Planform

In this section x_t and θ_L are defined by the inputs L, W and R. Then, the combination of L, W and R that meet the $x_t \geq 3.0$ feet and $\theta_L \leq 38°$ requirements are found, and used in the next steps. Specifically, these are used as bounds in a simplified cubic spine formula.

4.2.1 Wedge-curve

In the initial geometry development the input three variables: Length (L), Width(W), Transition point from the line to the curve before the DUT area (X_t), were taken as the independent variables. The length on the X-axis and correlate with 25 feet quite zone dimension. The width variable lay along the Y-axis and correlated with the 20 feet long quiet zone. The transition point from the line to the curve before the DUT area lay on the X-axis. After solving for these three variables the final equation was a transcendental equation which was incompatible with the FEKO(R) geometry scripting construct.

To avoid the transcendental equation the transition point from the line to the curve before the DUT area (X_t) was replaced with Radius of the Curve (R). The origin of the curve is on the Y-axis and position on the Y-axis varies with the size of width and the radius. So,the Radius of the Curve determines the angle (θ_{look}), and transition point (X_t) at a particular width. The result is a purely algebraic expression, compatible with the geometry generation program.

4.2.2 Finding X_t, Y_t and θ_L and Suitable Combinations of Input Values

The following formulas for X_t, Y_t and θ_L are derived with respect to the inputs L, W, and R. Then, the combinations of L, W, and R that meet the $x_t \geq 3.0$ feet and $\theta_L \leq 38°$ requirements are extracted. The formula for the cubic spline is derived based on the resulting end and control points.

4.2.2.1 Solving for the X_t, Y_t and θ_L Value

Because of the transcendental equation when using the the values L, W, and X_t, X_t was replaced with R. To find X_t it is advisable to first find y_0 which is the origin of the radius of R which must lie on the Y-axis. This value is found by Equation (3)

$$y_0 = W - R \tag{3}$$

Since the objective is to solve for x_t and y_t, two equation are needed. The first equation is simply the Pythagorean theorem as shown in equation Equation (4). Then solving for y_t follows algebraically as shown in equation Equation (5).

$$x_t^2 + (y_t - y_0)^2 = R^2 \tag{4}$$

$$y_t = \sqrt{R^2 - x_t^2} + y_0 \tag{5}$$

The second equation matches the slope of the line to the slope of the circle at any given point on the circle, and is defined as shown in equation Equation (6).

$$\frac{dy}{dx} = \frac{d}{dx}\left[\left(R^2 - x_t^2\right)^{\frac{1}{2}} + y_0\right] = \frac{-x_t}{\sqrt{R^2 - x_t^2}} \tag{6}$$

At the point L on the X-axis, the slope has the same tangent as the circle that intersects with at x_t, y_t, as shown in Equation (7). The result may be substituted into the slope, m_t the circle from Equation (6) and then into Equation (7) to arrive at Equation (8).

$$y_t = m_t\left(x_t - L\right) \tag{7}$$

$$y_t = \left(\frac{-x_t}{\sqrt{R^2 - x_t^2}}\right)\left(x_t - L\right) \tag{8}$$

Equation (5) and Equation (8) are set equal to each other based on the equality of y_t as shown in Equation (9). x_t may then be solved for, as shown in Equation (10) through Equation (13).

$$\sqrt{R^2 - x_t^2} + y_0 = \left(\frac{-x_t}{\sqrt{R^2 - x_t^2}}\right)\left(x_t - L\right) \tag{9}$$

$$R^2 - x_t^2 + y_0\sqrt{R^2 - x_t^2} = -x_t\left(x_t - L\right) \tag{10}$$

$$y_0\sqrt{R^2 - x_t^2} = x_t^2 + Lx_t - R^2 + x_t^2 \tag{11}$$

$$\sqrt{R^2 - x_t^2} = \frac{L}{y_0}x_t - \frac{R^2}{y_0} \tag{12}$$

$$R^2 - x_t^2 = \left(\frac{L}{y^0}\right)^2 x_t^2 - 2\left(\frac{L}{y_0}\right)\left(\frac{R^2}{y_0}\right)x_t + \left(\frac{R^4}{y_0^2}\right) \tag{13}$$

The resulting equation is a 2^{nd} order root search, as shown in Equation (14).

$$\left[\left(\frac{L}{y_0}\right)^2 + 1\right]x_t^2 + \left[\frac{-2LR^2}{y_0^2}\right]x_t + \left[\frac{R^4}{y_0^2} - R^2\right] = 0 \tag{14}$$

By using the quadratic equation this low order systemcan be solved for x_t as shown in Equation (15)

$$x_t = \frac{\left[\frac{2LR^2}{y_0^2}\right] \pm \sqrt{\left[\frac{-2LR^2}{y_0^2}\right]^2 - 4\left[\left(\frac{L}{y^0}\right)^2 + 1\right]\left[\frac{R^4}{y_0^2} - R^2\right]}}{2\left[\left(\frac{L}{y_0}\right)^2 + 1\right]} \tag{15}$$

By simplifying Equation (15) and restricting attention to the positive case, x_t yields Equation (16). This equation is used to solve for x_t given the other input variables.

$$x_t = \frac{LR^2 + y_0R\sqrt{L_2 - y_0^2 - R^2}}{L^2 + y_0^2} \tag{16}$$

With x_t solved as a function of the inputs of L, W, and R, y_t can be solved using Equation (5).

With both x_t and y_t solved for with respect to the inputs L, W, and R, θ_{look} can be solved for by 90-θ_L, where θ_L is the internal half angle found by using Equation (17).

For simplicity θ_L will be used for the following calculations.

$$\theta_L = arctan\left(\frac{y_t}{L - x_t}\right) \tag{17}$$

4.2.3 Radius and Straight

Now that x_t and θ_L are known with respect to the inputs L, W, and R, the next step is to determine which combinations of L, W & R meet the $x_t \geq$3.0 feet requirement. Similarly, the values for which $\theta_L \leq 38°$ are assessed. Two different lengths are evaluated, the first being the full size of the quiet zone which makes L = 12.5 ft and the second a 20% smaller example for the which L = 10.

Table 3 shows W and R combination with L = 10, values that meet $\theta_L \leq 38°$ which are highlighted by green cells. Table 4 shows W and R combination with L = 10 where $x_t \geq$3.0 feet are highlighted in the green cells. The trade space of moving x_t closer to DUT, is highlighted by yellow cells where $2.6 \leq x_t < 3.0$ and orange cells where $2.5 \leq x_t < 2.6$

Table 5 is a logical AND between Table 3 and Table 4. Cells that do not meet both requirements have a 'False' value in the cell and are highlighted in red. Cells that meet both requirement have a 'True' in the cell and have the same color coding as Table 4.

Table 3: θ_L when Length (L) is 10 feet. Green highlighted cells show combinations of Width (W) and Radius (R) at are $\theta_L \leq 38°$

L (ft)	W (ft)	R (ft)									
		3.75	4.00	4.25	4.50	4.75	5.00	5.25	5.50	5.75	6.00
10	6	34.1	34.4	34.7	35.0	35.2	35.5	35.9	36.2	36.5	36.9
10	6.25	35.4	35.7	35.9	36.2	36.5	36.9	37.2	37.6	37.9	38.3
10	6.5	36.6	36.9	37.2	37.5	37.8	38.2	38.5	38.9	39.3	39.7
10	6.75	37.7	38.1	38.4	38.7	39.1	39.4	39.8	40.2	40.6	41.0
10	7	38.9	39.2	39.6	39.9	40.3	40.7	41.1	41.5	41.9	42.4
10	7.25	40.0	40.4	40.7	41.1	41.5	41.9	42.3	42.7	43.2	43.7
10	7.5	41.1	41.5	41.8	42.2	42.6	43.1	43.5	43.9	44.4	44.9
10	7.75	42.2	42.6	42.9	43.3	43.8	44.2	44.7	45.1	45.6	46.2
10	8	43.2	43.6	44.0	44.4	44.9	45.3	45.8	46.3	46.8	47.3
10	8.25	44.2	44.6	45.0	45.5	45.9	46.4	46.9	47.4	47.9	48.5
10	8.5	45.2	45.6	46.1	46.5	47.0	47.4	48.0	48.5	49.0	49.6
10	8.75	46.2	46.6	47.0	47.5	48.0	48.5	49.0	49.5	50.1	50.7
10	9	47.1	47.5	48.0	48.5	48.9	49.5	50.0	50.6	51.2	51.8
10	9.25	48.0	48.4	48.9	49.4	49.9	50.4	51.0	51.6	52.2	52.8
10	9.5	48.9	49.3	49.8	50.3	50.8	51.4	51.9	52.5	53.1	53.8
10	9.75	49.7	50.2	50.7	51.2	51.7	52.3	52.8	53.4	54.1	54.7
10	10	50.5	51.0	51.5	52.0	52.6	53.1	53.7	54.3	55.0	55.7

Legend
$38° \leq \theta_L$

Table 4: x_t when Length (L) is 10 feet. Green highlighted cells show combinations of Width (W) and Radius (R) are $x_t \geq 3.0$. Yellow highlighted cells are $2.6 \leq x_t < 3.0$. Orange highlighted cells are $2.5 \leq x_t < 2.6$.

L (ft)	W (ft)	R (ft)									
		3.75	4.00	4.25	4.50	4.75	5.00	5.25	5.50	5.75	6.00
10	6	2.10	2.26	2.42	2.58	2.74	2.91	3.08	3.25	3.42	3.60
10	6.25	2.17	2.33	2.49	2.66	2.83	3.00	3.17	3.35	3.53	3.72
10	6.5	2.23	2.40	2.57	2.74	2.91	3.09	3.27	3.45	3.64	3.83
10	6.75	2.30	2.47	2.64	2.81	2.99	3.18	3.36	3.55	3.74	3.94
10	7	2.35	2.53	2.71	2.89	3.07	3.26	3.45	3.64	3.84	4.04
10	7.25	2.41	2.59	2.77	2.96	3.15	3.34	3.53	3.73	3.94	4.14
10	7.5	2.47	2.65	2.84	3.02	3.22	3.41	3.61	3.82	4.02	4.24
10	7.75	2.52	2.71	2.90	3.09	3.29	3.49	3.69	3.90	4.11	4.33
10	8	2.57	2.76	2.95	3.15	3.35	3.55	3.76	3.98	4.19	4.41
10	8.25	2.62	2.81	3.01	3.21	3.41	3.62	3.83	4.05	4.27	4.49
10	8.5	2.66	2.86	3.06	3.26	3.47	3.68	3.90	4.12	4.34	4.57
10	8.75	2.70	2.91	3.11	3.32	3.53	3.74	3.96	4.18	4.41	4.64
10	9	2.75	2.95	3.16	3.37	3.58	3.80	4.02	4.25	4.48	4.71
10	9.25	2.79	2.99	3.20	3.42	3.63	3.85	4.08	4.31	4.54	4.78
10	9.5	2.82	3.03	3.25	3.46	3.68	3.91	4.13	4.36	4.60	4.84
10	9.75	2.86	3.07	3.29	3.51	3.73	3.95	4.18	4.42	4.66	4.90
10	10	2.90	3.11	3.33	3.55	3.77	4.00	4.23	4.47	4.71	4.95

Legend
$3.0 \leq x_t$
$2.6 \leq x_t < 3.0$
$2.5 \leq x_t < 2.6$

Table 5: $\theta_L \leq 38°$ and x_t when Length (L) is 10 feet. Cells with 'TRUE' are $x_t \geq 2.5$ AND $\theta_L \leq 38°$. Green highlighted cells show combinations of Width (W) and Radius (R) are $x_t \geq 3.0$. Yellow highlighted cells are $2.6 \leq x_t < 3.0$. Orange highlighted cells are $2.5 \leq x_t < 2.6$.

L (ft)	W (ft)	R (ft)									
		3.75	4.00	4.25	4.50	4.75	5.00	5.25	5.50	5.75	6.00
10	6	FALSE	FALSE	FALSE	TRUE	TRUE	TRUE	TRUE	TRUE	TRUE	TRUE
10	6.25	FALSE	FALSE	FALSE	TRUE	TRUE	TRUE	TRUE	TRUE	TRUE	FALSE
10	6.5	FALSE	FALSE	TRUE	TRUE	TRUE	FALSE	FALSE	FALSE	FALSE	FALSE
10	6.75	FALSE	FALSE	FALSE	FALSE	FALSE	FALSE	FALSE	FALSE	FALSE	FALSE
10	7	FALSE	FALSE	FALSE	FALSE	FALSE	FALSE	FALSE	FALSE	FALSE	FALSE
10	7.25	FALSE	FALSE	FALSE	FALSE	FALSE	FALSE	FALSE	FALSE	FALSE	FALSE
10	7.5	FALSE	FALSE	FALSE	FALSE	FALSE	FALSE	FALSE	FALSE	FALSE	FALSE
10	7.75	FALSE	FALSE	FALSE	FALSE	FALSE	FALSE	FALSE	FALSE	FALSE	FALSE
10	8	FALSE	FALSE	FALSE	FALSE	FALSE	FALSE	FALSE	FALSE	FALSE	FALSE
10	8.25	FALSE	FALSE	FALSE	FALSE	FALSE	FALSE	FALSE	FALSE	FALSE	FALSE
10	8.5	FALSE	FALSE	FALSE	FALSE	FALSE	FALSE	FALSE	FALSE	FALSE	FALSE
10	8.75	FALSE	FALSE	FALSE	FALSE	FALSE	FALSE	FALSE	FALSE	FALSE	FALSE
10	9	FALSE	FALSE	FALSE	FALSE	FALSE	FALSE	FALSE	FALSE	FALSE	FALSE
10	9.25	FALSE	FALSE	FALSE	FALSE	FALSE	FALSE	FALSE	FALSE	FALSE	FALSE
10	9.5	FALSE	FALSE	FALSE	FALSE	FALSE	FALSE	FALSE	FALSE	FALSE	FALSE
10	9.75	FALSE	FALSE	FALSE	FALSE	FALSE	FALSE	FALSE	FALSE	FALSE	FALSE
10	10	FALSE	FALSE	FALSE	FALSE	FALSE	FALSE	FALSE	FALSE	FALSE	FALSE

Legend
$3.0 \leq x_t$ *AND* $38° \leq \theta_L$
$2.6 \leq x_t < 3.0$ *AND* $38° \leq \theta_L$
$2.5 \leq x_t < 2.6$ *AND* $38° \leq \theta_L$

Table 5 shows that there are only a few combinations of L, W and R that satisfy both $x_t \geq 3.0$ AND $\theta_L \leq 38°$ requirements. In Table 4 over half of the combinations of L, W, and R satisfy $x_t \geq 3.0$, however in Table 5 there are few combinations of L, W, and R that satisfy $\theta_L \leq 38°$, which limits the Width to 6.25 ft. This severely limits the 5 wavelength requirement.

Table 6 shows W and R combinations for L = 12.5, wjere values that meet $\theta_L \leq 38°$ are highlighted by green cells. Table 7 shows W and R combinations for L = 12.5 where $x_t \geq 3.0$ feet are green cells. To highlight the trade-off of moving x_t closer to DUT, yellow cells where $2.6 \leq x_t < 3.0$ and orange cells are $2.5 \leq x_t < 2.6$ are color coded.

Table 8 is logical AND between Table 6 and Table 7. Cells that do not meet both requirements have a 'False' in the cell and are highlighted in red. Cells that meet both requirement have a 'True' in the cell and have the same color coding as Table 7.

Table 6: θ_L when Length (L) is 12.5 feet. Green highlighted cells show combinations of Width (W) and Radius (R) at are $\theta_L \leq 38°$

L (ft)	W (ft)	R (ft)									
		3.75	4.00	4.25	4.50	4.75	5.00	5.25	5.50	5.75	6.00
12	6	28.5	28.7	28.8	29.0	29.1	29.3	29.5	29.6	29.8	30.0
12	6.25	29.6	29.7	29.9	30.1	30.2	30.4	30.6	30.8	31.0	31.2
12	6.5	30.6	30.8	31.0	31.2	31.4	31.5	31.7	31.9	32.1	32.3
12	6.75	31.7	31.9	32.1	32.2	32.4	32.6	32.8	33.1	33.3	33.5
12	7	32.7	32.9	33.1	33.3	33.5	33.7	33.9	34.2	34.4	34.6
12	7.25	33.7	33.9	34.1	34.3	34.6	34.8	35.0	35.3	35.5	35.8
12	7.5	34.7	34.9	35.1	35.4	35.6	35.8	36.1	36.3	36.6	36.9
12	7.75	35.7	35.9	36.1	36.4	36.6	36.9	37.1	37.4	37.7	37.9
12	8	36.6	36.9	37.1	37.4	37.6	37.9	38.1	38.4	38.7	39.0
12	8.25	37.6	37.8	38.1	38.3	38.6	38.9	39.1	39.4	39.7	40.0
12	8.5	38.5	38.7	39.0	39.3	39.5	39.8	40.1	40.4	40.7	41.1
12	8.75	39.4	39.6	39.9	40.2	40.5	40.8	41.1	41.4	41.7	42.1
12	9	40.3	40.5	40.8	41.1	41.4	41.7	42.0	42.4	42.7	43.0
12	9.25	41.1	41.4	41.7	42.0	42.3	42.6	42.9	43.3	43.6	44.0
12	9.5	42.0	42.3	42.6	42.9	43.2	43.5	43.8	44.2	44.6	44.9
12	9.75	42.8	43.1	43.4	43.7	44.0	44.4	44.7	45.1	45.5	45.8
12	10	43.6	43.9	44.2	44.5	44.9	45.2	45.6	46.0	46.3	46.7

Legend
$\theta_L \leq 38°$

Table 7: x_t when Length (L) is 12.5 feet. Green highlighted cells show combinations of Width (W) and Radius (R) are $x_t \geq 3.0$. Yellow highlighted cells are $2.6 \leq x_t < 3.0$. Orange highlighted cells are $2.5 \leq x_t < 2.6$.

L (ft)	W (ft)	R (ft)									
		3.75	4.00	4.25	4.50	4.75	5.00	5.25	5.50	5.75	6.00
12.5	6	1.72	1.85	1.97	2.10	2.22	2.35	2.48	2.61	2.75	2.88
12.5	6.25	1.78	1.91	2.04	2.17	2.30	2.44	2.57	2.71	2.84	2.98
12.5	6.5	1.84	1.98	2.11	2.24	2.38	2.52	2.66	2.80	2.94	3.09
12.5	6.75	1.90	2.04	2.18	2.31	2.46	2.60	2.74	2.89	3.04	3.19
12.5	7	1.96	2.10	2.24	2.38	2.53	2.68	2.82	2.98	3.13	3.28
12.5	7.25	2.01	2.16	2.30	2.45	2.60	2.75	2.90	3.06	3.22	3.38
12.5	7.5	2.06	2.21	2.36	2.52	2.67	2.83	2.98	3.14	3.30	3.47
12.5	7.75	2.12	2.27	2.42	2.58	2.74	2.90	3.06	3.22	3.39	3.56
12.5	8	2.17	2.32	2.48	2.64	2.80	2.97	3.13	3.30	3.47	3.64
12.5	8.25	2.21	2.37	2.54	2.70	2.87	3.03	3.20	3.38	3.55	3.73
12.5	8.5	2.26	2.43	2.59	2.76	2.93	3.10	3.27	3.45	3.63	3.81
12.5	8.75	2.31	2.47	2.64	2.81	2.99	3.16	3.34	3.52	3.70	3.89
12.5	9	2.35	2.52	2.69	2.87	3.04	3.22	3.40	3.59	3.77	3.96
12.5	9.25	2.39	2.57	2.74	2.92	3.10	3.28	3.47	3.65	3.84	4.03
12.5	9.5	2.44	2.61	2.79	2.97	3.15	3.34	3.53	3.72	3.91	4.11
12.5	9.75	2.48	2.66	2.84	3.02	3.21	3.39	3.59	3.78	3.97	4.17
12.5	10	2.52	2.70	2.88	3.07	3.26	3.45	3.64	3.84	4.04	4.24

Legend
$3.0 \leq x_t$
$2.6 \leq x_t < 3.0$
$2.5 \leq x_t < 2.6$

Table 8: $\theta_L \leq 38°$ and x_t when Length (L) is 12.5 feet. Cells with 'TRUE' are $x_t \geq 2.5$ AND $\theta_L \leq 38°$. Green highlighted cells show combinations of Width (W) and Radius (R) are $x_t \geq 3.0$. Yellow highlighted cells are $2.6 \leq x_t < 3.0$. Orange highlighted cells are $2.5 \leq x_t < 2.6$.

L (ft)	W (ft)	R (ft)									
		3.75	4.00	4.25	4.50	4.75	5.00	5.25	5.50	5.75	6.00
12.5	6	FALSE	FALSE	FALSE	FALSE	FALSE	FALSE	FALSE	TRUE	TRUE	TRUE
12.5	6.25	FALSE	FALSE	FALSE	FALSE	FALSE	FALSE	TRUE	TRUE	TRUE	TRUE
12.5	6.5	FALSE	FALSE	FALSE	FALSE	FALSE	TRUE	TRUE	TRUE	TRUE	TRUE
12.5	6.75	FALSE	FALSE	FALSE	FALSE	FALSE	TRUE	TRUE	TRUE	TRUE	TRUE
12.5	7	FALSE	FALSE	FALSE	FALSE	TRUE	TRUE	TRUE	TRUE	TRUE	TRUE
12.5	7.25	FALSE	FALSE	FALSE	FALSE	TRUE	TRUE	TRUE	TRUE	TRUE	TRUE
12.5	7.5	FALSE	FALSE	FALSE	TRUE	TRUE	TRUE	TRUE	TRUE	TRUE	TRUE
12.5	7.75	FALSE	FALSE	FALSE	TRUE	TRUE	TRUE	TRUE	TRUE	TRUE	TRUE
12.5	8	FALSE	FALSE	FALSE	TRUE	TRUE	TRUE	FALSE	FALSE	FALSE	FALSE
12.5	8.25	FALSE	FALSE	FALSE	FALSE	FALSE	FALSE	FALSE	FALSE	FALSE	FALSE
12.5	8.5	FALSE	FALSE	FALSE	FALSE	FALSE	FALSE	FALSE	FALSE	FALSE	FALSE
12.5	8.75	FALSE	FALSE	FALSE	FALSE	FALSE	FALSE	FALSE	FALSE	FALSE	FALSE
12.5	9	FALSE	FALSE	FALSE	FALSE	FALSE	FALSE	FALSE	FALSE	FALSE	FALSE
12.5	9.25	FALSE	FALSE	FALSE	FALSE	FALSE	FALSE	FALSE	FALSE	FALSE	FALSE
12.5	9.5	FALSE	FALSE	FALSE	FALSE	FALSE	FALSE	FALSE	FALSE	FALSE	FALSE
12.5	9.75	FALSE	FALSE	FALSE	FALSE	FALSE	FALSE	FALSE	FALSE	FALSE	FALSE
12.5	10	FALSE	FALSE	FALSE	FALSE	FALSE	FALSE	FALSE	FALSE	FALSE	FALSE

Legend
$3.0 \leq x_t$ $AND\ \theta_L \leq 38^{\circ}$
$2.6 \leq x_t < 3.0\ AND\ \theta_L \leq 38^{\circ}$
$2.5 \leq x_t < 2.6\ AND\ \theta_L \leq 38^{\circ}$

Early full wave simulations, based on these dimensional pairings, demonstrated that the results were more angularly narrowly confined than predicted by PO methods. So, the θ_L value was increased to 40°, as indicated in table 9, values that are $\theta_L \leq 40°$ are shown in green cells.

Table 10 is logical AND between Table 9 and Table 7. Cells that do not meet both requirements have a 'False' in cell and are red cells. Cells that meet both requirement have a 'True' in the cell and have the same color coding as Table 7.

Table 9: θ_L when Length (L) is 12.5 feet. Green highlighted cells show combinations of Width (W) and Radius (R) at are $\theta_L \leq 40°$

L (ft)	W (ft)	R (ft)									
		3.75	4.00	4.25	4.50	4.75	5.00	5.25	5.50	5.75	6.00
12.5	6	27.4	27.5	27.6	27.8	27.9	28.1	28.2	28.4	28.5	28.7
12.5	6.25	28.4	28.6	28.7	28.9	29.0	29.2	29.3	29.5	29.7	29.8
12.5	6.5	29.4	29.6	29.8	29.9	30.1	30.2	30.4	30.6	30.8	31.0
12.5	6.75	30.5	30.6	30.8	31.0	31.1	31.3	31.5	31.7	31.9	32.1
12.5	7	31.5	31.6	31.8	32.0	32.2	32.4	32.5	32.7	33.0	33.2
12.5	7.25	32.4	32.6	32.8	33.0	33.2	33.4	33.6	33.8	34.0	34.2
12.5	7.5	33.4	33.6	33.8	34.0	34.2	34.4	34.6	34.8	35.1	35.3
12.5	7.75	34.3	34.5	34.8	35.0	35.2	35.4	35.6	35.9	36.1	36.4
12.5	8	35.3	35.5	35.7	35.9	36.2	36.4	36.6	36.9	37.1	37.4
12.5	8.25	36.2	36.4	36.6	36.9	37.1	37.4	37.6	37.9	38.1	38.4
12.5	8.5	37.1	37.3	37.6	37.8	38.0	38.3	38.6	38.8	39.1	39.4
12.5	8.75	38.0	38.2	38.5	38.7	39.0	39.2	39.5	39.8	40.1	40.4
12.5	9	38.8	39.1	39.3	39.6	39.9	40.1	40.4	40.7	41.0	41.3
12.5	9.25	39.7	39.9	40.2	40.5	40.7	41.0	41.3	41.6	41.9	42.3
12.5	9.5	40.5	40.8	41.1	41.3	41.6	41.9	42.2	42.5	42.8	43.2
12.5	9.75	41.3	41.6	41.9	42.2	42.5	42.8	43.1	43.4	43.7	44.1
12.5	10	42.1	42.4	42.7	43.0	43.3	43.6	43.9	44.3	44.6	44.9

Legend
$\theta_L \leq 40°$

Table 10: $\theta_L \leq 40°$ and x_t when Length (L) is 12.5 feet. Cells with 'TRUE' are $x_t \geq 2.5$ AND $\theta_L \leq 40°$. Green highlighted cells show combinations of Width (W) and Radius (R) are $x_t \geq 3.0$. Yellow highlighted cells are $2.6 \leq x_t < 3.0$. Orange highlighted cells are $2.5 \leq x_t < 2.6$.

L (ft)	W (ft)	R (ft)									
		3.75	4.00	4.25	4.50	4.75	5.00	5.25	5.50	5.75	6.00
12.5	6	FALSE	FALSE	FALSE	FALSE	FALSE	FALSE	FALSE	TRUE	TRUE	TRUE
12.5	6.25	FALSE	FALSE	FALSE	FALSE	FALSE	FALSE	TRUE	TRUE	TRUE	TRUE
12.5	6.5	FALSE	FALSE	FALSE	FALSE	FALSE	TRUE	TRUE	TRUE	TRUE	TRUE
12.5	6.75	FALSE	FALSE	FALSE	FALSE	FALSE	TRUE	TRUE	TRUE	TRUE	TRUE
12.5	7	FALSE	FALSE	FALSE	FALSE	TRUE	TRUE	TRUE	TRUE	TRUE	TRUE
12.5	7.25	FALSE	FALSE	FALSE	FALSE	TRUE	TRUE	TRUE	TRUE	TRUE	TRUE
12.5	7.5	FALSE	FALSE	FALSE	TRUE	TRUE	TRUE	TRUE	TRUE	TRUE	TRUE
12.5	7.75	FALSE	FALSE	FALSE	TRUE	TRUE	TRUE	TRUE	TRUE	TRUE	TRUE
12.5	8	FALSE	FALSE	FALSE	TRUE	TRUE	TRUE	TRUE	TRUE	TRUE	TRUE
12.5	8.25	FALSE	FALSE	TRUE	TRUE	TRUE	TRUE	TRUE	TRUE	TRUE	TRUE
12.5	8.5	FALSE	FALSE	TRUE	TRUE	TRUE	TRUE	TRUE	TRUE	TRUE	TRUE
12.5	8.75	FALSE	FALSE	TRUE	TRUE	TRUE	TRUE	TRUE	TRUE	FALSE	FALSE
12.5	9	FALSE	TRUE	TRUE	TRUE	TRUE	FALSE	FALSE	FALSE	FALSE	FALSE
12.5	9.25	FALSE	TRUE	FALSE	FALSE	FALSE	FALSE	FALSE	FALSE	FALSE	FALSE
12.5	9.5	FALSE	FALSE	FALSE	FALSE	FALSE	FALSE	FALSE	FALSE	FALSE	FALSE
12.5	9.75	FALSE	FALSE	FALSE	FALSE	FALSE	FALSE	FALSE	FALSE	FALSE	FALSE
12.5	10	FALSE	FALSE	FALSE	FALSE	FALSE	FALSE	FALSE	FALSE	FALSE	FALSE

Legend
$3.0 \leq x_t$ $AND\ \theta_L \leq 40°$
$2.6 \leq x_t < 3.0\ AND\ \theta_L \leq 40°$
$2.5 \leq x_t < 2.6\ AND\ \theta_L \leq 40°$

Table 10 show that the allowable dimensions for the L = 12.5 start as low as W = 6.5 ft with a R = 6.0 ft and with a maximum W = 9.0 ft with a R = 4.75 ft. As the width (W) increases the radius (R) decreases for combinations of L, W and R set the limits of $x_t \geq 3.0$ AND $\theta_L \leq 40°$.

4.2.4 2^{nd} Derivative Continuous Shape Profile

An alternative upper geometry shape to the straight-radius is a second derivative continuous spline. The 2^{nd} derivative continuous equation, which is a cubic spline under certain limitations, is required for geometry definition based on the inputs of L and W from the straight curve in order to set up a comparison of similar sizes planform objects for Radar Cross-Section (RCS) performance.

The equation for a cubic spline through four points is given in Equation (18).

The equation for a cubic spline through four points is dependent upon the following variables. $\overline{A}$ is 4-by-4 matrix, Equation (19) and uses the x-coordinate pairs of (x_1, y_1), (x_2, y_2), (x_3, y_3), (x_4, y_4). $\overline{x}$ is a 4-by-1 matrix of the unknown coefficient, Equation (20). $\overline{B}$ is a 4-by-1 matrix, Equation (21). The cubic spline through four points is given in Equation (18). When all of the values are substituted, the full matrix is given Equation (22)

$$\overline{A}\overline{x} = \overline{B} \tag{18}$$

$$\overline{A} = \begin{bmatrix} x_1^3 & x_1^2 & x_1 & 1 \\ x_2^3 & x_2^2 & x_2 & 1 \\ x_3^3 & x_3^2 & x_3 & 1 \\ x_4^3 & x_3^2 & x_4 & 1 \end{bmatrix} \tag{19}$$

$$\overline{x} = \begin{bmatrix} a \\ b \\ c \\ d \end{bmatrix} \tag{20}$$

$$\overline{B} = \begin{bmatrix} y_1 \\ y_2 \\ y_3 \\ y_4 \end{bmatrix} \tag{21}$$

$$\begin{bmatrix} x_1^3 & x_1^2 & x_1 & 1 \\ x_2^3 & x_2^2 & x_2 & 1 \\ x_3^3 & x_3^2 & x_3 & 1 \\ x_4^3 & x_3^2 & x_4 & 1 \end{bmatrix} \begin{bmatrix} a \\ b \\ c \\ d \end{bmatrix} = \begin{bmatrix} y_1 \\ y_2 \\ y_3 \\ y_4 \end{bmatrix} \tag{22}$$

The four point for the spline are (-L, 0), $(-x_s,\ y_s)$, $(x_s,\ y_s)$, (L, 0). x_s is equal to 0.1 and y_s is equal to W. The four points are substituted into Equation (22) and solved for $\overline{x}$ yielding the functional result shown in Equation (23). The resulting function is sufficient for a bounded geometry definition in FEKO.

$$f(x) = \left(\frac{-y_s}{L^2 - x_s^2} \right) x^2 + \left(\frac{L^2 y_s}{L^2 - x_s^2} \right) \tag{23}$$

4.3 Shape Comparison

A comparison of radius straight and the spline plate RCS results is executed to determine which shape best meets the requirements. The common size for the comparison will start with the radius straight dimensions and that L and W will determine the spline dimensions. This allows a comparison design based on the them having the same size. The upper and lower frequencies will be used to evaluate the RCS of the designs. The radius straight will best meet the given requirements.

4.3.1 Geometric Definitions for Comparison

The basic comparison is between the radius straight geometry defined by equations (eq. (16), eq. (17)) and the combinations of inputs L, W & R that fit within the bounds of $x_t \geq 3.0$ and $\theta_L \leq 40°$, Table 10, and the geometry defined by cubic spline equations (eq. (23)), with L, $x_s = .1$ and $y_s =$ W. The radius straight values that will be used are L = 12.5 ft, W = 8.25 ft, R = 5.5 ft and L = 10.0 ft, W = 6 ft, R = 6.5 ft, Figure 8.

With this structure in place an evaluation of which shape performs best for the requirements was conducted. First, the radius straight case was selected and those dimensions used to create the cubic spline by eq. (23). The importance of selecting the wedge curve first and then using those dimensions for the cubic spline is to retain the five wavelength requirement from the edge to the DUT area. This yields a valid comparison between the geometry profiles. To facilitate analysis the upper and lower limit of the frequency band was used, which are 500 MHz and 2000 MHz.

Geometric Optics (GO) was helpful in finding the angle to avoid the main lobe however because DUT is the focus of this design the surface current contributions can be significant, so a Computational Electromagnetics (CEM) method is need to calculate and include the surface currents traveling on the test fixture in the far field scattering. The most common method is the Method of Moments (MoM), which requires N^2 memory which can be easy exceeded the computer's memory. To address this problem for large meshes Multilevel Fast Multipole Method (MLFMM) was used, which reduces the memory requirement form N^2 to $N \log N$. This allows for large mesh sizes than would not work with a pure method.

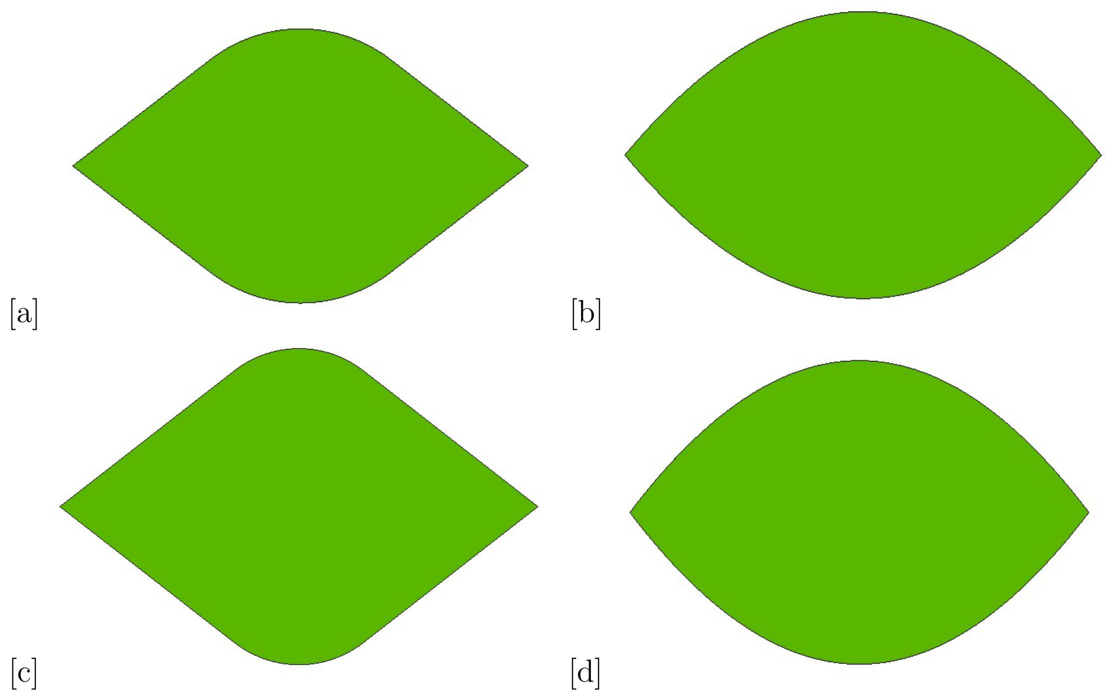

Figure 8: Geometry comparison between radius straight versus spline design and Length of L = 10 ft versus L = 12.5 ft. (a) Radius/Straight L = 10.0, W = 6.0, R = 6.5 (b) Spline L = 10.0, W = 6.0 (c) Radius/Straight L = 12.5, W = 8.25, R= 5.5 (d) Spline L = 12.5, W = 8.25

4.3.2 Radius Straight versus Spline shape

The electromagnetic wave orientation it is noted by the way the wave travels. When electromagnetic wave travels up and down is known as vertical polarization and when it side to side is known as horizontal orientation. This orientation can also be noted in a spherical coordinate system where the vertical orientation of the electric field is known by Theta and the horizontal orientation of the electric field is noted by Phi. When the electrical wave is sent out in the vertical orientation and is observed in the vertical orientation this is known as Theta Theta (tt). The wave leaves the radar in the Theta direction and is observing it in the Theta direction. Likewise when the electrical wave is sent out in the horizontal orientation and is observed in the horizontal orientation this is known as Phi Phi (pp). The wave leaves the radar in the Phi direction and is observing it in the Phi direction. tt and pp with be used to evaluate RCS performance

The comparison used the theta-theta polarization (tt-pol) and all profiles had a plate profile and depth of 1.2 ft to ensure that the response of the shape was observable in the returns. The difference between the radius/straight and the cubic spline with a L = 12.5 ft at 500MHz, as shown in Figure 9 and L = 10.0 at 500 and 2000 MHz, Figure 10 are systematic and significant. As may be observed in both figures, the spikes for the cubic spline occurred within or at the 45 degrees limits while the spikes for the radius/straight occurred outside the 45 degree window. To quantify the difference in the two shape designs, RCS performance was calculated for the 500MHz and 2000MHz cases. Table 11 shows the PCUM 50 and PCUM 90 values over angles in dBsm.

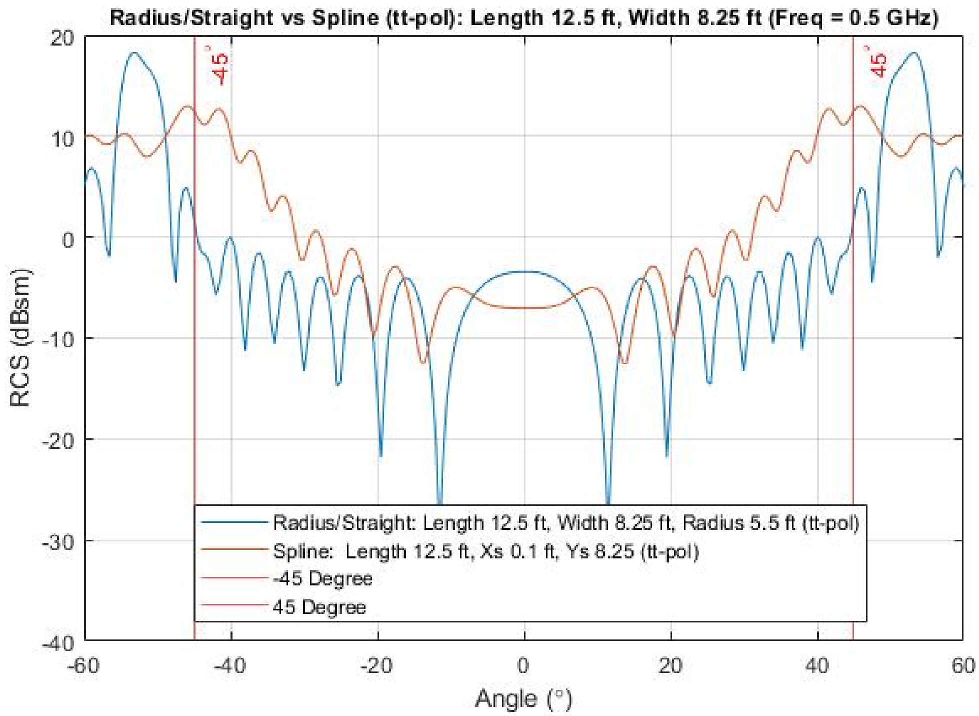

Figure 9: RCS of radius straight versus spline design at 500MHz with L = 12.5 ft and W = 8.25 ft. The spline RCS spikes at the 45°, while the radius straight RCS spikes are outside -45° thru 45° measurement zone.

Table 11: RCS values of radius straight vs spline shape for 500MHz and 2000MHz with L= 12.5 and L = 10.0 showing PCUM50 and PCUM90 in dB.

	Shape	L=12.5ft, W= 8.25 (tt-pol) Frequency (MHz)		L=10.0ft, W= 6.0 (tt-pol) Frequency (MHz)	
		500.0	2000.0	500.0	2000.0
PCUM 50	Radius & Straight	-5.08	-9.36	-5.20	-9.38
PCUM 50	Spline	-3.82	-5.43	-2.92	-6.29
PCUM 90	Radius & Straight	-2.40	-4.60	-2.62	-4.40
PCUM 90	Spline	10.09	16.83	6.55	12.05

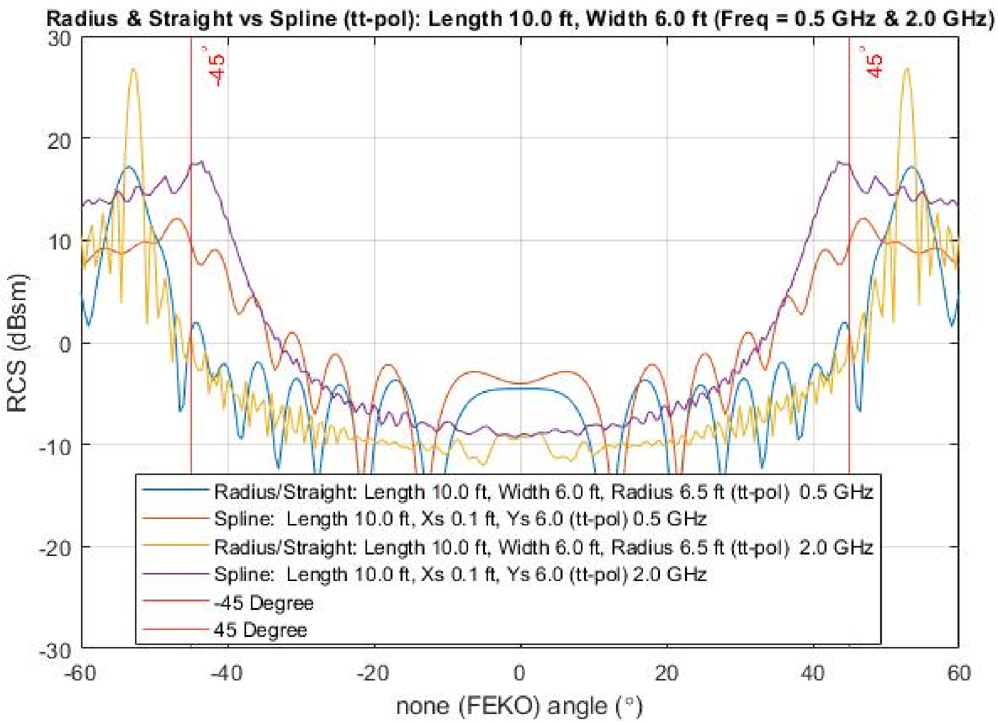

Figure 10: RCS of radius straight versus spline design at 500MHz and 2000 MHz with L = 10 ft ane W = 6.0 ft. The spline RCSs spikes at the 45°, while the radius straight RCSs spikes are outside -45° thru 45° measurement zone.

As seen in Figure 9 and Figure 10 the RCS from the spline design spiked at the +/-45°, while the radius straight design spike was outside the -45° thru 45° measurement zone. This observation was further validated by Table 11 by showing that the PCUM50s and PCUM90s of the spline design had higher RCS values than the radius straight design.

4.4 Bounds on Total Geometry by Spline Nose Angle

The spline is a second derivative continuous curve which has a moving specular point. Because of this specular scattering component, energy cannot be consolidated in angularly narrow spikes as efficiently as in the radius-straight case. However, the steep angle of concern is the the tangent line from nose of the spline, shown in Figure 11. Figure 12 demonstrates how varying the width affects the tangent line from the nose when L = 12.5. To constrain the tangent line angle to be $\theta_L \leq 40°$ induces a requirement that W $\leq$ 5.75 ft, which is 3 ft smaller than 8.75 for the width of the radius/straight shape. The tangent line of the nose for L = 10.0, is shown in Figure 13, and is even worse with $\theta_L \leq 40°$ when W $\leq$ 3.5 ft which is only 1 ft away from the DUT. The spikes move when varying the width when L = 12.5 as shown in Figure 14. The plot for W = 5.25 appears similar to the radius/straight plot with W = 8.25. as shown in Figure 9 in

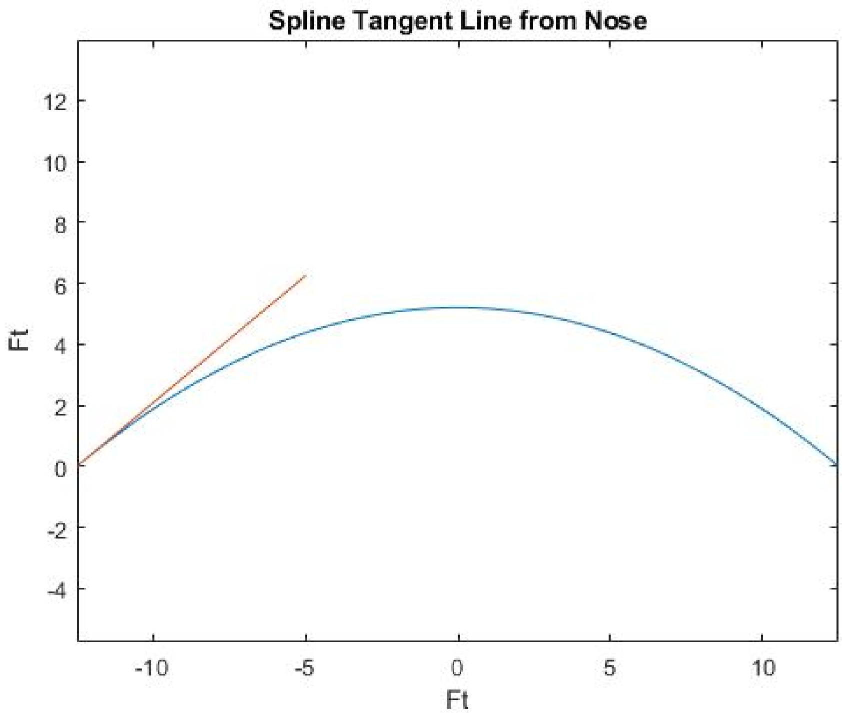

Figure 11: Spline tangent line (Red) from nose is the steepest angle along the spline curve and is the reference point for the worst return

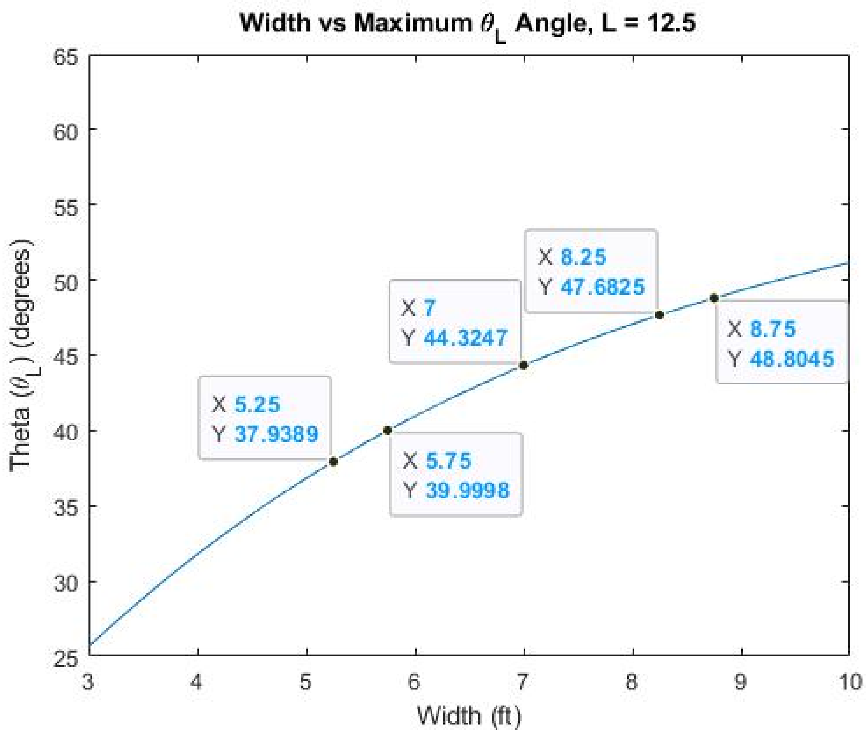

Figure 12: Spline tangent line angle from nose θ_L vs width with L = 12.5 ft. Highlighting key widths (x values) and the tangent nose angle (y values). When the W = 8.25 ft the tangent nose angle is 47.7°. To get a tangent nose angle of 38° like the radius straight design the width is 5.25 ft.

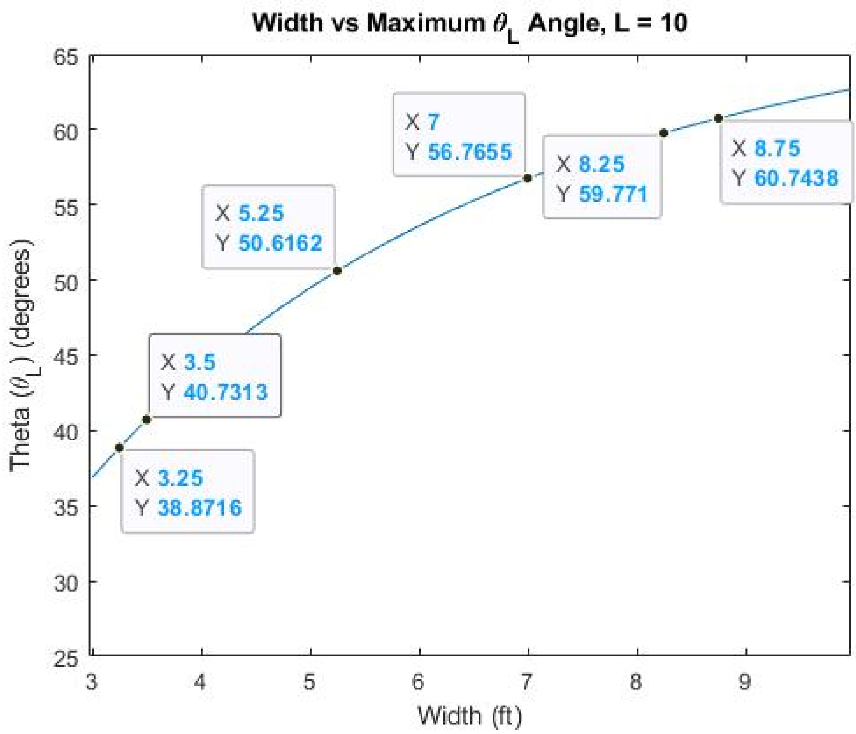

Figure 13: Spline tangent line angle from nose θ_L vs width with L = 10.0 ft. Highlighting key widths (x values) and the tangent nose angle (y values). When the W = 5.25 ft the tangent nose angle is 50.6°. To get a tangent nose angle of 38° like the radius straight design the width is 3.25 ft.

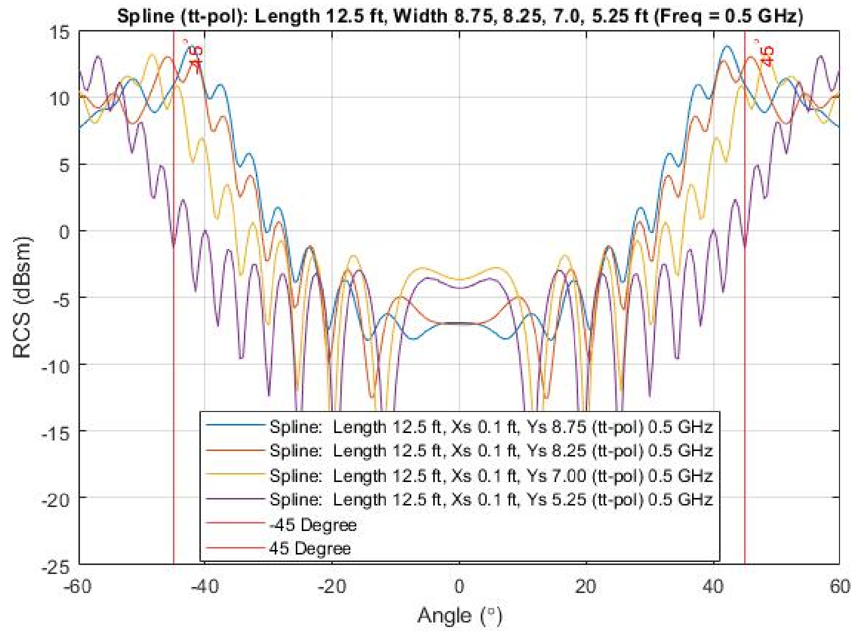

Figure 14: RCS of spline design at L = 12.5 ft with W = 8.75, 8.25, 7.0, 5.25 ft at 500MHz. The spline RCS spikes for the W = 5.25 has a similar spike as the radius straight with a W = 8.25, shown in Figure 9.

The spline has a low RCS in the nose area, however to get a similar response with the spikes outside the -45° thru 45° measurement zone the width must be greatly reduced losing the similar shape as to the radius straight design which give the radius straight design the advantage because it has a much larger 5 wavelength distance.

4.5 Postamble

In this section the formulas of x_t, Equation (16), and θ_L, Equation (17), with respects to the inputs L W R were derived fro geometry generation. Next, L, W and R input combinations were found that satisfied both $x_t \geq 3.0$ and $\theta_L \leq 40°$. the results are shown in Table 10. Then the equation for the cubic spline was solved for in terms of L, x_s, y_s, Equation (23), where L = L, $x_s = 0.1$, and y_s = W. Then, a comparison was made between the radius straight to the cubic spline with the results in Table 11 showing that the radius straight design has a lower PCUM values in every area. Figures 11 to 14 shows that to get similar response with the spikes outside the -45° thru 45° measurement zone the width of the spline must be greatly reduced.

The radius straight with L = 12.5 ft is the selected the best design, because the radius straight had smaller PCUM values than the spline design, as shown in Table 11. Also, the radius straight with L = 12.5 ft has a larger width, as shown in Table 10, than radius straight with L = 10.0 ft, as shown in Table 5

V. Test Surface MoM Based Design Refinement

5.1 Preamble

In this section the down-select from the radius/straight and the cubic spline to a final upper surface geometry shape is completed. Next, a range of frequencies are selected for optimization and testing. With the final shape and frequencies selected, five size parameter sets are selected for sector data and PCUM date extraction which bound the edges and center of a geometry derived response surface. Then the RCS values of the five sizes are calculated for comparison with the five wavelength decay calculations for each frequency from the edge to the Device Under Test (DUT). Lastly, the final size selection will be made by developing a cost function the for the PCUM data and DUT 5 wavelength data decay data.

5.2 Upper/Lower Frequency Cross Check and Geometry Down Select

The comparison of the radius straight to the cubic spline, yields the following results. The radius/straight with a length of 12.5 ft has a width of 8.75 ft, which is gives a distance of 6.25 ft to DUT. The lowest frequency that has 5 wavelength of setback is 787MHz and at 500MHz there are only 3.175 wavelengths of setback. This does fall below the requirement, but it is the best that can be done with respect to the quiet zone restrictions. The spline that has a length of 12.5 and a width of 8.75 produces a signature spike in the 45°, as shown in Figure 14. To move the spikes outside 45° the width would have to be 5.75 ft, as shown in Figure 12. This would give a setback distance of 3.25 ft to the DUT. The lowest frequency that has 5 wavelength of setback is 1514MHz and at 500MHz there are only 1.65 wavelengths of setback. As a result of this spike impingement, the radius/straight also has lower PCUM50 and PCUM90 values, as shown in Table 11.

The radius/straight geometry is selected because it out performs the cubic spline form in both the PCUM50 and PCUM90 metrics and provides the largest setback distance from the edge to DUT. Therefore, the remainder of this work further refines the radius straight upper surface geometry.

5.3 Selection of Frequencies to Run Based on Spectrum Edges

To speed up the process of selecting the top surface shape the upper and lower frequencies were used to make the evaluation of which shape to pursue. With the radius straight shape selected, using the upper and lower frequencies would be inadequate for optimization algorithms and for determining the best size of the selected shape for overall Radar Cross-Section (RCS) results over the band. Instead of using a simple linear selection of frequencies, a more nuanced set of test frequencies was found, based on the Department of Defense (DoD) spectrum allocations that are between 500MHz and 2GHz. This information was found in DoD Strategic Spectrum Plan, February 2008 [12]. In October 2008 there was DoD Electromagnetic Spectrum Superiority Strategy, follow up by several revision through October 2020, however document did not list band edge frequencies in the document, so the DoD Strategic Spectrum Plan, from February 2008 was used [13]. Even though this document is not current this is somewhat trivial because, the Federal Communications Commission (FCC) Allocation History File tracks the changes made to the frequency allocations. The only changes that were made to the 500 - 2000 MHz range since the publication of the DoD Strategic Spectrum Plan, February 2008, was in the 900MHz and only to 896-901 MHz and 935-940 MHz GSM cellular bands, which are not part of the military frequencies, per Table 12 [14].

In Table 12 are all the military frequencies bands that are between 500 - 2000MHz and the frequency bands that are just outside of focus area area listed and a description of the use of the band is given. All bands have center frequency assigned to each band, except the bands that are in the 900MHz, because of the small bandwidth, the 3 bandwidths are combined and given one center frequency. The Delta (MHz) column in Table 12 shows the difference for the previous center frequency to the current center frequency. Delta ranges from 70 to 432 MHz.

Table 12: DoD frequencies band edges used in the 500 - 2000MHz range and missions that used that frequency. The center frequency for each frequency band and the delta between the center frequencies. 900MHz band are combined into on one band with one center frequency [12].

Lower Frequency (MHz)	Upper Frequency (MHz)	Center Frequency (MHz)	Delta (MHz)	Description of frequency use:
420	450	NA	NA	Voice/Data, LMR, EPLRS, 2D Air Search, Airborne Early Warning (AEW), Space Surveillance, EW Training, Command Control Link
500		500	0	Start of Range
902	928			2D Air Search, Target Acquisition, NAVAIDS, Shipboard Air Defense, Command Control Link, Test Range Operations
932	935	923.000	423.0	Voice/Data, Air Defense Radar, Radiolocation, Command Control Link
941	944			Voice/Data, Air Surveillance Radar, Command Control Link, AFRTS Audio/Visual
960	1215	1087.500	164.5	Voice/Data, JTIDS/MIDS, Command Control Link, ATC, Secondary Surveillance Radar, TACAN, Aircraft IFF, Long Range Radar
1215	1390	1302.500	215.0	Voice/Data, Command Control Link, ATC/NAVAIDS, Range & Test Operations, GPS, ICBM Detection/Surveillance Radar, Long-Medium Air Defense Radar, Training Range Operations
1390	1710	1550.000	247.5	Voice/Data, ATM, Low-Altitude Aircraft Detection, Precision Guided Munitions, Command Control Link, RDT&E
1710	1755	1732.500	182.5	Voice/Data, Data/Video Links, CIDDS, Range Telemetry, Precision Guided Munitions, Air Combat Training
1755	1850	1802.500	70.0	Voice/Data, Data/Video Links, CIDDS, Range Telemetry, Precision Guided Munitions, Space Operations, Air Combat Training
2000		2000	197.5	End of Range
2200	2290	NA	NA	SGLS, Telemetry, TeleCommand Control Link

This method of using the lower and upper frequencies in the frequency band to find the center frequency, as shown in the 3rd column of Table 12, which are then used for testing purposes yields greater utility than a linear span because the focus of this work is to test and optimize over the frequencies that the antennas will be used in and select the best parameters to decrease the RCS of the test fixture over these frequency bands. This analysis contributes in a non-trivial fashion to the overall value of the design process, and should be extended and/or applied to other test fixture designs.

5.4 Five Point Test Establishment

With the top shape surface selected and the frequencies selected for analysis, the next step is to find the optimum fixture size for the frequencies selected. Five analysis points were selected: one on each corner and on one in the middle of the geometry derived response surface. The two points at the lower end occur at W = 7 ft and the two points at the higher end occur at W = 8.75 ft. With the four points on top and bottom, two will yield $x_t < 3.0$ (green) and the other two will be $2.6 \leq x_t < 3.0$ (yellow), while the fifth one was centered. When the corners are connected there is a parallelogram, Figure 15, over which performance is expected to vary in a generally functional manner. Therefore, This search will nominally cover the different size combinations of interest and suggest which area will yield the best results. By considering marginal cases, a greater viable trade space is explored against DUT setback requirements.

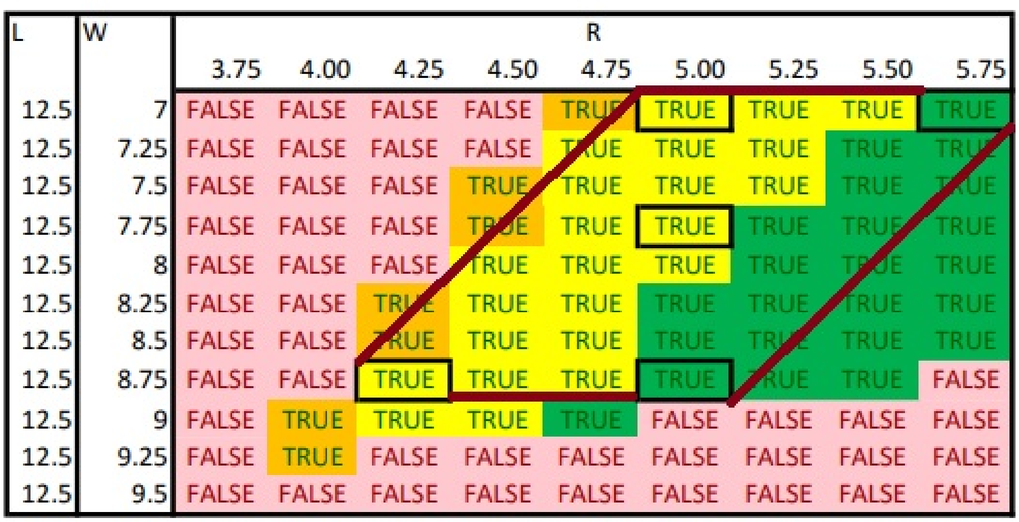

L	W	R								
		3.75	4.00	4.25	4.50	4.75	5.00	5.25	5.50	5.75
12.5	7	FALSE	FALSE	FALSE	FALSE	TRUE	TRUE	TRUE	TRUE	TRUE
12.5	7.25	FALSE	FALSE	FALSE	FALSE	TRUE	TRUE	TRUE	TRUE	TRUE
12.5	7.5	FALSE	FALSE	FALSE	TRUE	TRUE	TRUE	TRUE	TRUE	TRUE
12.5	7.75	FALSE	FALSE	FALSE	TRUE	TRUE	TRUE	TRUE	TRUE	TRUE
12.5	8	FALSE	FALSE	FALSE	TRUE	TRUE	TRUE	TRUE	TRUE	TRUE
12.5	8.25	FALSE	FALSE	TRUE	TRUE	TRUE	TRUE	TRUE	TRUE	TRUE
12.5	8.5	FALSE	FALSE	TRUE	TRUE	TRUE	TRUE	TRUE	TRUE	TRUE
12.5	8.75	FALSE	FALSE	TRUE	TRUE	TRUE	TRUE	TRUE	TRUE	FALSE
12.5	9	FALSE	TRUE	TRUE	TRUE	TRUE	FALSE	FALSE	FALSE	FALSE
12.5	9.25	FALSE	TRUE	FALSE	FALSE	FALSE	FALSE	FALSE	FALSE	FALSE
12.5	9.5	FALSE	FALSE	FALSE	FALSE	FALSE	FALSE	FALSE	FALSE	FALSE

Figure 15: 5 test point chart. Two points have W = 7.0 ft and two have a W = 8.75 ft. Both have one point where $x_t \geq 3.0$ (green boxes) and the another pint is $2.6 \leq x_t < 3.0$ (yellow boxes). The Last point is in the middle.

5.4.1 Sector Data and PCUMs

For each of the five dimension sets at the eight different frequencies, the RCS was calculated, as well as the PCUM50-tt, PCUM50-pp, PCUM90-tt and PCUM90-pp statics for each frequency. The results are tabulated in Tables 13 to 16 and graphically depicted in Figures 16 and 17.

Table 13: Five Point PCUM50-tt at the eight different frequencies in dB.

PCUM50-tt					
Frequency (MHz)	L = 12.5 W = 7.0 R = 5.75	L = 12.5 W = 7.0 R = 5.0	L = 12.5 W = 8.0 R = 5.0	L = 12.5 W = 8.75 R = 5.0	L = 12.5 W = 8.75 R = 4.25
500.0	-5.59	-5.69	-5.49	-5.20	-5.00
922.3	-9.14	-9.99	-8.71	-8.67	-9.01
1087.5	-7.25	-7.07	-8.33	-7.66	-7.86
1302.5	-7.82	-7.50	-8.44	-7.55	-8.63
1550.0	-3.49	-6.62	-7.62	-6.00	-6.83
1732.5	-2.61	-2.15	-7.59	-5.25	-5.97
1802.5	-5.04	-6.14	-6.22	-5.83	-6.74
2000.0	-4.66	3.75	-3.37	-2.07	-3.15

Table 14: Five Point PCUM50-pp at the eight different frequencies in dB.

PCUM50-pp					
Frequency (MHz)	L = 12.5 W = 7.0 R = 5.75	L = 12.5 W = 7.0 R = 5.0	L = 12.5 W = 8.0 R = 5.0	L = 12.5 W = 8.75 R = 5.0	L = 12.5 W = 8.75 R = 4.25
500.0	-14.94	-14.97	-15.66	-14.29	-14.70
922.3	-14.13	-15.10	-11.82	-15.38	-15.55
1087.5	-10.70	-10.53	-10.62	-9.24	-10.09
1302.5	-8.72	-9.62	-11.01	-9.68	-10.01
1550.0	-8.89	-7.85	-10.14	-7.97	-7.97
1732.5	-7.89	-5.48	-7.39	-6.19	-6.12
1802.5	-7.03	-7.03	-6.41	-4.49	-6.49
2000.0	-2.70	0.07	-1.21	-0.03	-2.43

The tabulated results do not reveal a size combination that yields exceptionally superior performance, although the trends run as expected. Therefore, the consider-

Table 15: Five Point PCUM90-tt at the eight different frequencies in dB.

PCUM90-tt					
Frequency (MHz)	L = 12.5 W = 7.0 R = 5.75	L = 12.5 W = 7.0 R = 5.0	L = 12.5 W = 8.0 R = 5.0	L = 12.5 W = 8.75 R = 5.0	L = 12.5 W = 8.75 R = 4.25
500.0	-3.66	-3.63	-3.35	-1.65	-2.15
922.3	-7.00	-7.39	-6.16	-3.72	-4.97
1087.5	-3.92	-3.76	-4.35	-3.23	-3.88
1302.5	-5.17	-3.34	-4.27	-1.81	-2.94
1550.0	1.94	-2.80	-2.20	-1.92	-2.31
1732.5	0.63	1.50	-4.32	-0.79	-1.38
1802.5	-1.15	-1.23	-1.54	-0.47	-2.55
2000.0	1.32	7.28	6.66	3.81	2.80

Table 16: Five Point PCUM90-pp at the eight different frequencies in dB.

PCUM90-pp					
Frequency (MHz)	L = 12.5 W = 7.0 R = 5.75	L = 12.5 W = 7.0 R = 5.0	L = 12.5 W = 8.0 R = 5.0	L = 12.5 W = 8.75 R = 5.0	L = 12.5 W = 8.75 R = 4.25
500.0	-6.69	-6.41	-5.96	-4.05	-3.44
922.3	-6.17	-6.32	-6.44	-4.08	-5.69
1087.5	-5.12	-5.48	-4.88	-4.44	-2.96
1302.5	-5.25	-4.98	-5.35	-3.43	-4.56
1550.0	-4.42	-2.96	-2.54	-1.86	-2.40
1732.5	-2.19	-0.37	-1.85	-0.28	0.95
1802.5	-0.95	-2.81	-0.38	1.11	0.21
2000.0	4.79	7.01	7.98	8.59	3.57

[a]

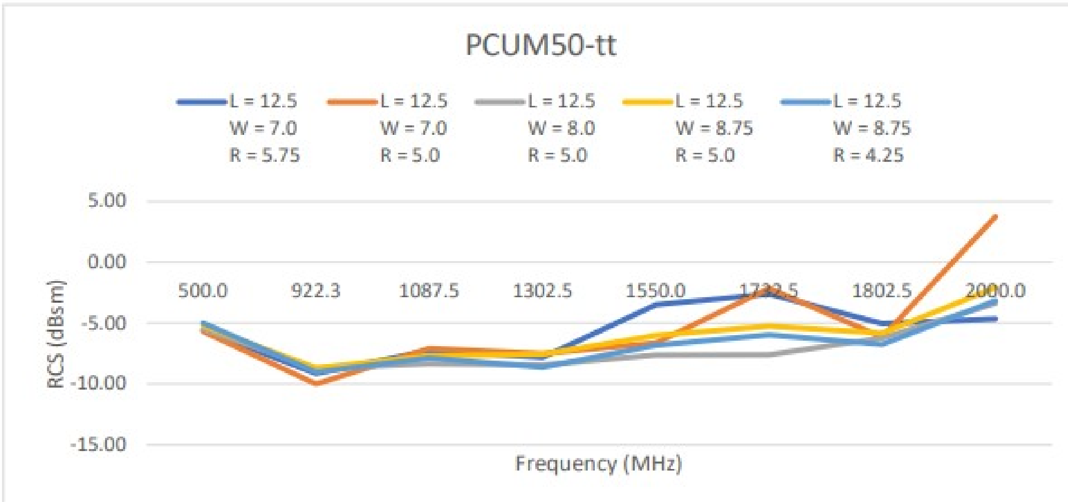

[b]

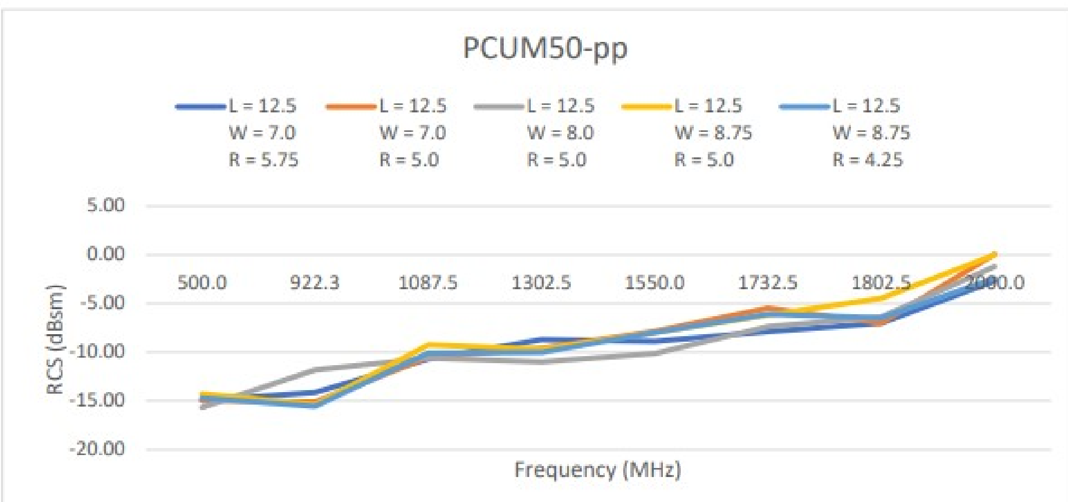

Figure 16: Five point PCUM50 RCS plots for the eight frequnecies: (a) PCUM50-tt (b) PCUM50-pp

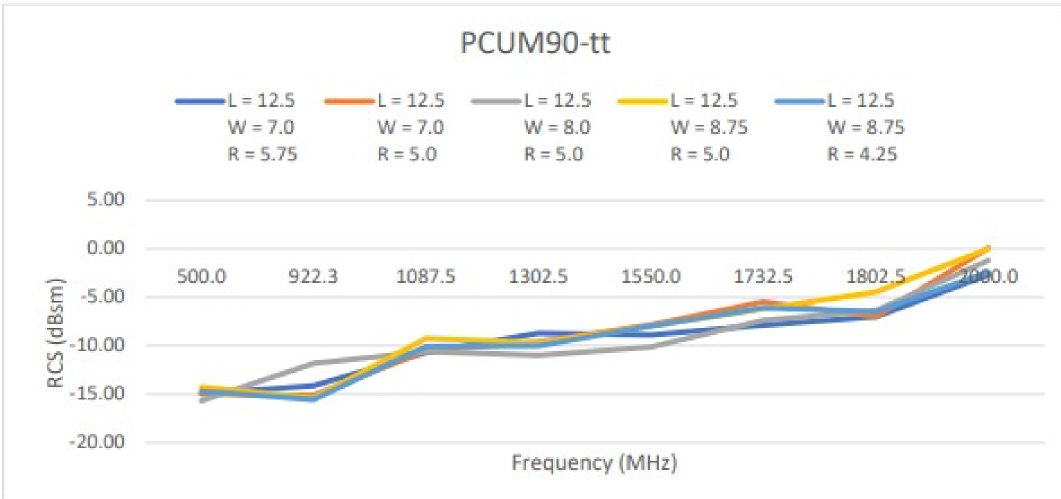

[a]

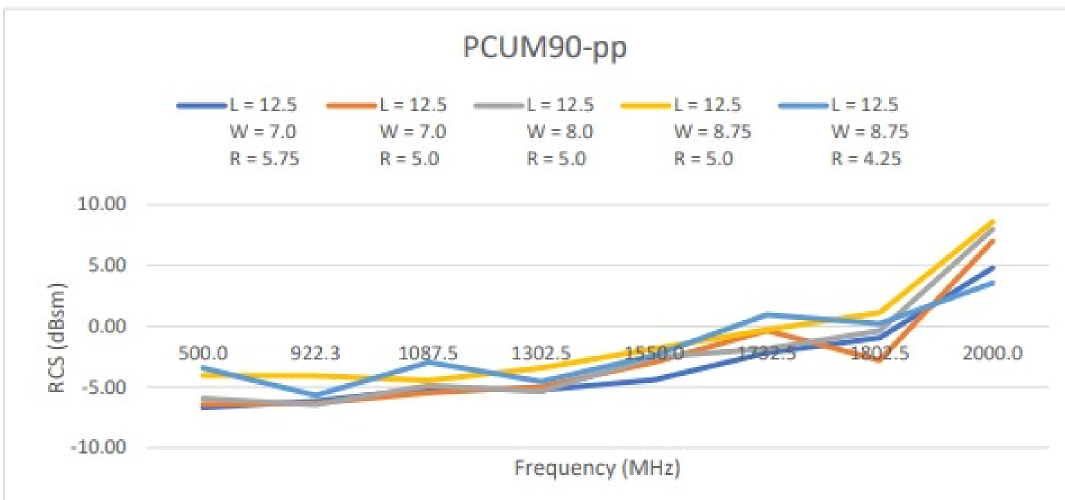

[b]

Figure 17: Five point PCUM90 RCS plots for the eight frequnecies: (a) PCUM90-tt (b) PCUM90-pp

ation of surface wave decay cannot be truncated in finalizing the design. Rather, a formalized comparison must be made.

5.5 DUT 5 Wave Decay Calculation By Frequency

The requirement for the five wavelength distance is based on moving the fixture edge out of the most active near field of the antenna, and is a function of frequency. The lower the frequency the longer the wavelength, per Equation (1). Five wavelength of setback from the edge to the DUT is based on a rule of thumb that goes back to the exponential decay, e^{-x}. Generally, five decay coefficients will yield a trivial level, and Table 17 shows that when x = 5 that 99.3% decay has occurred. This approximation is valid, in as much as the decay coefficient goes as a wavelength of distance.

Table 17: Exponential decay for 1/lambda decay constant from -1 to -5. Showing the percent decay.

x	Exponenetial Decay (eˆx)	Decay (%)
1	0.3679	-63.20%
2	0.1353	-86.50%
3	0.0498	-95.00%
4	0.0183	-98.20%
5	0.0067	-99.30%

The lowest frequency is 500MHz which has wavelength of 1.97 ft. Out of the five different sizes there are only three different widths: 7, 8 and 8.75 ft. Table 18 shows the distance from the edge to the DUT, the frequency needed to get five wavelengths of setback, how many 500MHz wavelengths fits in the given distance and the 500MHz exponential decay.

The analysis is across frequencies, so the decay for all eight frequencies for each of the three different widths is required. The number of wavelengths for each frequency

Table 18: Edge to DUT distance vs decay for 500MHz and the frequency need to satisfy the five wavelength requirement.

Width (ft)	DUT (ft)	distance (ft)	Frequency that is 5 wavelength (MHz)	# wavelength at 500MHz	Exponential decay for 500MHz	Remaining after 500MHz Decay (%)
7.00	2.5	4.5	1094	2.29	0.102	10.2%
8.00	2.5	5.5	895	2.79	0.061	6.1%
8.75	2.5	6.25	787	3.18	0.042	4.2%

are calculated and substituted in the exponential decay formula. The exponential decay is then converted to dB by $10log_{10}$ and the results for each frequency at each width, are given in Table 19.

Table 19: dB decay per edge to DUT distances per frequencies. the number of wavelengths for a particular frequency and distance, which is then used to calculate the decay and the decay is then put into a $10log_{10}$ to calculate the dB decay

Frequency (MHz)	Width (ft)	DUT (ft)	Number of wavelength (λ)	Decay	LOG decay (dB)
500.0	7.00	2.5	2.29	0.10167234	-9.9
500.0	8.00	2.5	2.79	0.06117602	-12.1
500.0	8.75	2.5	3.18	0.04179410	-13.8
922.3	7.00	2.5	4.22	0.01474978	-18.3
922.3	8.00	2.5	5.15	0.00577895	-22.4
922.3	8.75	2.5	5.86	0.00286185	-25.4
1087.5	7.00	2.5	4.97	0.00692893	-21.6
1087.5	8.00	2.5	6.08	0.00229517	-26.4
1087.5	8.75	2.5	6.91	0.00100213	-30.0
1302.5	7.00	2.5	5.96	0.00259277	-25.9
1302.5	8.00	2.5	7.28	0.00069031	-31.6
1302.5	8.75	2.5	8.27	0.00025586	-35.9
1550.0	7.00	2.5	7.09	0.00083624	-30.8
1550.0	8.00	2.5	8.66	0.00017314	-37.6
1550.0	8.75	2.5	9.84	0.00005314	-42.7
1732.5	7.00	2.5	7.92	0.00036304	-34.4
1732.5	8.00	2.5	9.68	0.00006245	-42.0
1732.5	8.75	2.5	11.00	0.00001668	-47.8
1802.5	7.00	2.5	8.24	0.00026361	-35.8
1802.5	8.00	2.5	10.07	0.00004223	-43.7
1802.5	8.75	2.5	11.45	0.00001069	-49.7
2000.0	7.00	2.5	9.14	0.00010686	-39.7
2000.0	8.00	2.5	11.18	0.00001401	-48.5
2000.0	8.75	2.5	12.70	0.00000305	-55.2

5.6 Cost/Quality Function Development to Weight Upper Surface Geometrical Bounds in RCS Sector Data vs Decay

There are two different but important metrics that need to be considered. One is the RCS values in Section 5.4.1 and second the five wavelength decay in Section 5.5. On one side of the trade space is having a low RCS, which usually corresponds with the smaller shape. On the other side is five wavelengths of decay, which serves to reduce the near field effect from the edge of the test fixture and have near field effects decay significantly before the DUT. This usually corresponds with the results from a larger shape and is in conflict with the low RCS requirement.

There was no requirement set regarding to how to compare the dB decay to the dBsm values from the RCS calcuations. So, both are normalized to the same frequency data and given the same weight then added together for that geometry.

Equation (24) was used to normalized RCS and the five wavelength. Some algebra is required to create a positive values representing the best results scaling. The lowest value in that frequency was x_{max} for that frequency and x_{min} is 10, because no values are greater than 10. The lowest negative value was x_{max}, and large positive valuess are desired. Both normalized value are multiple by 0.5 and added together to create a combined benefit function. Table 20 is an example of the calculation for PCUM50-tt, while Table 21 shows all the finalized values for all of the PCUMs cases.

$$x_{normalized} = \frac{(x - x_{min})}{(x_{max} - x_{min})} \tag{24}$$

Table 20: Normalized the RCS dB and the decay dB by using the normalized RCS dB and the decay dB. The lower value is desired, so, the lowest value in that frequency was x_{max} for that frequency and x_{min} is 10, because no values are greater than 10. With lowest negative value was x_{max}, this mean that large positive values are good. Both normalized value are multiple by 0.5 and added together

Size	Freq (MHz)	W (ft)	TUT (ft)	# (λ)	Decay	decay (dB)	X-max	X-min	Normal-ize per freq Decay	RCS dB	X-max	X-min	Normal-ize per freq RCS	Decay Weight	RCS Weight	Total
L=12.5,W= 7.0,R=5.75	500.0	7.00	2.5	2.29	0.1016723	-9.9	-13.8	10	0.84	-5.6	-5.7	10	0.99	0.5	0.5	0.916
L=12.5,W= 7.0,R=5.00	500.0	7.00	2.5	2.29	0.1016723	-9.9	-13.8	10	0.84	-5.7	-5.7	10	1.00	0.5	0.5	0.919
L=12.5,W= 8.0,R=5.00	500.0	8.00	2.5	2.79	0.0611760	-12.1	-13.8	10	0.93	-5.5	-5.7	10	0.99	0.5	0.5	0.959
L=12.5,W= 8.75,R=5.00	500.0	8.75	2.5	3.18	0.0417941	-13.8	-13.8	10	1.00	-5.2	-5.7	10	0.97	0.5	0.5	0.985
L=12.5,W= 8.75,R=4.25	500.0	8.75	2.5	3.18	0.0417941	-13.8	-13.8	10	1.00	-5.0	-5.7	10	0.96	0.5	0.5	0.978
L=12.5,W= 7.0,R=5.75	922.3	7.00	2.5	4.22	0.0147498	-18.3	-25.4	10	0.80	-9.1	-10.0	10	0.96	0.5	0.5	0.878
L=12.5,W= 7.0,R=5.00	922.3	7.00	2.5	4.22	0.0147498	-18.3	-25.4	10	0.80	-10.0	-10.0	10	1.00	0.5	0.5	0.900
L=12.5,W= 8.0,R=5.00	922.3	8.00	2.5	5.15	0.0057790	-22.4	-25.4	10	0.91	-8.7	-10.0	10	0.94	0.5	0.5	0.925
L=12.5,W= 8.75,R=5.00	922.3	8.75	2.5	5.86	0.0028618	-25.4	-25.4	10	1.00	-8.7	-10.0	10	0.93	0.5	0.5	0.967
L=12.5,W= 8.75,R=4.25	922.3	8.75	2.5	5.86	0.0028618	-25.4	-25.4	10	1.00	-9.0	-10.0	10	0.95	0.5	0.5	0.975
L=12.5,W= 7.0,R=5.75	1087.5	7.00	2.5	4.97	0.0069289	-21.6	-30.0	10	0.79	-7.2	-8.3	10	0.94	0.5	0.5	0.866
L=12.5,W= 7.0,R=5.00	1087.5	7.00	2.5	4.97	0.0069289	-21.6	-30.0	10	0.79	-7.1	-8.3	10	0.93	0.5	0.5	0.861
L=12.5,W= 8.0,R=5.00	1087.5	8.00	2.5	6.08	0.0022952	-26.4	-30.0	10	0.91	-8.3	-8.3	10	1.00	0.5	0.5	0.955
L=12.5,W= 8.75,R=5.00	1087.5	8.75	2.5	6.91	0.0010021	-30.0	-30.0	10	1.00	-7.7	-8.3	10	0.96	0.5	0.5	0.982
L=12.5,W= 8.75,R=4.25	1087.5	8.75	2.5	6.91	0.0010021	-30.0	-30.0	10	1.00	-7.9	-8.3	10	0.97	0.5	0.5	0.987
L=12.5,W= 7.0,R=5.75	1302.5	7.00	2.5	5.96	0.0025928	-25.9	-35.9	10	0.78	-7.8	-8.6	10	0.96	0.5	0.5	0.869
L=12.5,W= 7.0,R=5.00	1302.5	7.00	2.5	5.96	0.0025928	-25.9	-35.9	10	0.78	-7.5	-8.6	10	0.94	0.5	0.5	0.860
L=12.5,W= 8.0,R=5.00	1302.5	8.00	2.5	7.28	0.0006903	-31.6	-35.9	10	0.91	-8.4	-8.6	10	0.99	0.5	0.5	0.948
L=12.5,W= 8.75,R=5.00	1302.5	8.75	2.5	8.27	0.0002559	-35.9	-35.9	10	1.00	-7.6	-8.6	10	0.94	0.5	0.5	0.971
L=12.5,W= 8.75,R=4.25	1302.5	8.75	2.5	8.27	0.0002559	-35.9	-35.9	10	1.00	-8.6	-8.6	10	1.00	0.5	0.5	1.000
L=12.5,W= 7.0,R=5.75	1550.0	7.00	2.5	7.09	0.0008362	-30.8	-42.7	10	0.77	-3.5	-7.6	10	0.77	0.5	0.5	0.769
L=12.5,W= 7.0,R=5.00	1550.0	7.00	2.5	7.09	0.0008362	-30.8	-42.7	10	0.77	-6.6	-7.6	10	0.94	0.5	0.5	0.858
L=12.5,W= 8.0,R=5.00	1550.0	8.00	2.5	8.66	0.0001731	-37.6	-42.7	10	0.90	-7.6	-7.6	10	1.00	0.5	0.5	0.951
L=12.5,W= 8.75,R=5.00	1550.0	8.75	2.5	9.84	0.0000531	-42.7	-42.7	10	1.00	-6.0	-7.6	10	0.91	0.5	0.5	0.954
L=12.5,W= 8.75,R=4.25	1550.0	8.75	2.5	9.84	0.0000531	-42.7	-42.7	10	1.00	-6.8	-7.6	10	0.95	0.5	0.5	0.977
L=12.5,W= 7.0,R=5.75	1732.5	7.00	2.5	7.92	0.0003630	-34.4	-47.8	10	0.77	-2.6	-7.6	10	0.72	0.5	0.5	0.743
L=12.5,W= 7.0,R=5.00	1732.5	7.00	2.5	7.92	0.0003630	-34.4	-47.8	10	0.77	-2.1	-7.6	10	0.69	0.5	0.5	0.730
L=12.5,W= 8.0,R=5.00	1732.5	8.00	2.5	9.68	0.0000624	-42.0	-47.8	10	0.90	-7.6	-7.6	10	1.00	0.5	0.5	0.950
L=12.5,W= 8.75,R=5.00	1732.5	8.75	2.5	11.00	0.0000167	-47.8	-47.8	10	1.00	-5.3	-7.6	10	0.87	0.5	0.5	0.934
L=12.5,W= 8.75,R=4.25	1732.5	8.75	2.5	11.00	0.0000167	-47.8	-47.8	10	1.00	-6.0	-7.6	10	0.91	0.5	0.5	0.954
L=12.5,W= 7.0,R=5.75	1802.5	7.00	2.5	8.24	0.0002636	-35.8	-49.7	10	0.77	-5.0	-6.7	10	0.90	0.5	0.5	0.833
L=12.5,W= 7.0,R=5.00	1802.5	7.00	2.5	8.24	0.0002636	-35.8	-49.7	10	0.77	-6.1	-6.7	10	0.96	0.5	0.5	0.866
L=12.5,W= 8.0,R=5.00	1802.5	8.00	2.5	10.07	0.0000422	-43.7	-49.7	10	0.90	-6.2	-6.7	10	0.97	0.5	0.5	0.934
L=12.5,W= 8.75,R=5.00	1802.5	8.75	2.5	11.45	0.0000107	-49.7	-49.7	10	1.00	-5.8	-6.7	10	0.95	0.5	0.5	0.973
L=12.5,W= 8.75,R=4.25	1802.5	8.75	2.5	11.45	0.0000107	-49.7	-49.7	10	1.00	-6.7	-6.7	10	1.00	0.5	0.5	1.000
L=12.5,W= 7.0,R=5.75	2000.0	7.00	2.5	9.14	0.0001069	-39.7	-55.2	10	0.76	-4.7	-4.7	10	1.00	0.5	0.5	0.881
L=12.5,W= 7.0,R=5.00	2000.0	7.00	2.5	9.14	0.0001069	-39.7	-55.2	10	0.76	3.8	-4.7	10	0.43	0.5	0.5	0.595
L=12.5,W= 8.0,R=5.00	2000.0	8.00	2.5	11.18	0.0000140	-48.5	-55.2	10	0.90	-3.4	-4.7	10	0.91	0.5	0.5	0.905
L=12.5,W= 8.75,R=5.00	2000.0	8.75	2.5	12.70	0.0000031	-55.2	-55.2	10	1.00	-2.1	-4.7	10	0.82	0.5	0.5	0.912
L=12.5,W= 8.75,R=4.25	2000.0	8.75	2.5	12.70	0.0000031	-55.2	-55.2	10	1.00	-3.1	-4.7	10	0.90	0.5	0.5	0.949

5.6.1 Analysis and Explanation

The total RCS benefits function across frequencies was the final value to compared. With this caluculation there is a clear winner to select "L= 12.5, w= 8.75 and r 4.25". The clear second place is "L= 12.5, w= 8.0 and r 5.0". This shows that the closed the x_t is to the center the lower the dBsm.

Table 21: Normalized and weighted totals for RCS and decay are summed across the different frequenies for each size. The highest total is the best over all dimension for that PCUM.

PCUM50-tt decay	Frequency (MHz)								
Dimensions (ft)	500	922.25	1087.5	1302.5	1550	1732.5	1802.5	2000	Total
L = 12.5, W = 7.0, R = 5.75	0.92	0.88	0.87	0.87	0.77	0.74	0.83	0.88	6.75
L = 12.5, W = 7.0, R = 5.0	0.92	0.90	0.86	0.86	0.86	0.73	0.87	0.59	6.59
L = 12.5, W = 8.0, R = 5.0	0.96	0.92	0.96	0.95	0.95	0.95	0.93	0.91	7.53
L = 12.5, W = 8.75, R = 5.0	0.98	0.97	0.98	0.97	0.95	0.93	0.97	0.91	7.68
L = 12.5, W = 8.75, R = 4.25	0.98	0.98	0.99	1.00	0.98	0.95	1.00	0.95	7.82

PCUM50-pp decay	Frequency (MHz)								
Dimensions (ft)	500	922.25	1087.5	1302.5	1550	1732.5	1802.5	2000	Total
L = 12.5, W = 7.0, R = 5.75	0.94	0.89	0.92	0.84	0.88	0.91	0.90	0.89	7.17
L = 12.5, W = 7.0, R = 5.0	0.94	0.92	0.92	0.87	0.84	0.82	0.90	0.76	6.97
L = 12.5, W = 8.0, R = 5.0	0.99	0.86	0.97	0.97	0.98	0.95	0.94	0.88	7.53
L = 12.5, W = 8.75, R = 5.0	0.97	1.00	0.96	0.97	0.95	0.95	0.91	0.88	7.57
L = 12.5, W = 8.75, R = 4.25	0.98	1.00	0.99	0.98	0.95	0.95	0.98	0.99	7.81

PCUM90-tt decay	Frequency (MHz)								
Dimensions (ft)	500	922.25	1087.5	1302.5	1550	1732.5	1802.5	2000	Total
L = 12.5, W = 7.0, R = 5.75	0.95	0.93	0.89	0.92	0.67	0.70	0.82	0.89	6.76
L = 12.5, W = 7.0, R = 5.0	0.95	0.94	0.88	0.84	0.90	0.66	0.82	0.50	6.50
L = 12.5, W = 8.0, R = 5.0	0.98	0.94	0.96	0.94	0.93	0.98	0.90	0.61	7.24
L = 12.5, W = 8.75, R = 5.0	0.92	0.88	0.95	0.88	0.96	0.87	0.90	0.85	7.21
L = 12.5, W = 8.75, R = 4.25	0.94	0.93	0.98	0.93	0.98	0.90	1.00	0.92	7.58

PCUM90-pp decay	Frequency (MHz)								
Dimensions (ft)	500	922.25	1087.5	1302.5	1550	1732.5	1802.5	2000	Total
L = 12.5, W = 7.0, R = 5.75	0.95	0.93	0.89	0.92	0.67	0.70	0.82	0.89	6.76
L = 12.5, W = 7.0, R = 5.0	0.95	0.94	0.88	0.84	0.90	0.66	0.82	0.50	6.50
L = 12.5, W = 8.0, R = 5.0	0.98	0.94	0.96	0.94	0.93	0.98	0.90	0.61	7.24
L = 12.5, W = 8.75, R = 5.0	0.92	0.88	0.95	0.88	0.96	0.87	0.90	0.85	7.21
L = 12.5, W = 8.75, R = 4.25	0.94	0.93	0.98	0.93	0.98	0.90	1.00	0.92	7.58

5.6.2 Selection of Upper Surface Geometry Parameters

From an RCS perspective, the clear winner is the larger width and smaller the x_t value. The other consideration is the stand off distance form DUT, which is the same distance as the circle on the bottom of the fixture. This stand off distance is important because the RCS of the fixture which can't be reduce and may be removed through post-processing if is is identifiable. So, to compromise the L=12.5, W = 8.75, R = 5.0 were shifted to L=12.5, W = 8.75, R = 4.75 and this set of geometric parameters defines the finally upper surface to the test fixture.

5.7 Postamble

The radius straight geometry was selected over the spline shaped geometry. The tests frequencies were selected from the center frequencies of the bands used by the DoD between 500 - 2000MHz. Then five sizes were selected to compare RCS of the different frequencies. Next, the decay of five wavelength was calculated for each geometry size configuration. The RCS and five wavelength decay results were normalized, weighted, and summed together assess the multi-parameter performance. Then, the final design was selected based on the results.

VI. Overall 3-D Surface Method of Moments Based Design Refinement

6.1 Preamble

The top surface shape and size has been selected in the previous section. In this section, the lower fixture shape and is designed and optimized. This task requires teh finalized geometry parameters and method of moments mesh to be established. The requirements on the mesh are not explicitly part of the design requirements, and are explained. Then the angular resolution for the Radar Cross-Section (RCS) calculations are set, and the RCS data calculated. The final full Three Dimensions (3-D) design's performance is evaluated to access the overall results.

6.2 Lower Test Fixture Design

The lower test fixture profile is comprised of three segments. The first segment is a flat diagonal line that is defined by the chord, D, as the dimension coming in from the edge and D1 as the extending below the flat surface. The second segment is the flat surface that is directly underneath the Device Under Test (DUT) area which is required to have a radius equal to x_t. Finally, the third segment is the connection between the diagonal from the surface edge to the bottom flat surface. The requirement for this segment is that when the curve connects to both surfaces that the tangent of line at the connection point is the same as the trangent of the surface to which it connects. Also, the curvature is a second derivative continuous to reduce unnecessary returns.

6.2.1 Bézier Curve Definition

The Bézier curve has a convenient feature that accommodates the requirement that the tangent of the curve is equal to the targent of line that is connecting. The tangent at the starting point (point one) is created by the line between point one and point two. Likewise, the tangent at the ending point (point 4), is the tangent of the line between point 3 and point 4. This requires that point 2 be on the same plane as the plane that point 1 is connected to, achieve the correct tangent. This is the same for point 3 in that it must remain on the same plane as point 4. The variable parameter is the distance that point 2 is away from point 1 and point 3 distance from point 4, as shown in Figure 18

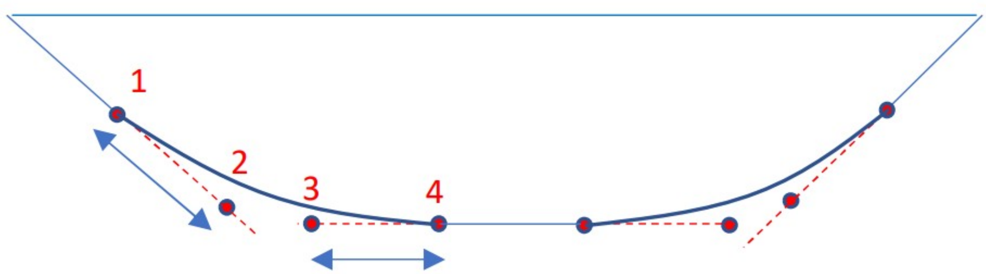

Figure 18: Bézier curve side view diagram for full 3-D lower geometry shows that point 2 and 3 is on the plain of point 1 and 4, which make the tangent of point 1 and 4 equal to the line tangents that they connect to.

This process must be repeated for both the tip to tip and side to side cases of the geometry. Due to the limited Computer-Aided Design (CAD) capability in Feko it was not possible to create the boat hull design without losing the variables connected to the shape precluding automatic optimization. The most viable solution was to conduct a secondary optimization by creating the shape from tip to tip and side to side and then extruding that results. The optimization was then conducted only for theta form -5° to 40° with 2.5° steps. The optimum values are tabulated in Table 22. Upon geometry generation, it was noted that the side bézier curves had a bulge which required that the bézier side variable be changed from 2.1355 to 1.75 to remove the bulge. The side bézier curves will only be viewed by the side viewed (0°) to the 45° and not straight on (90°) as it was in the optimization.

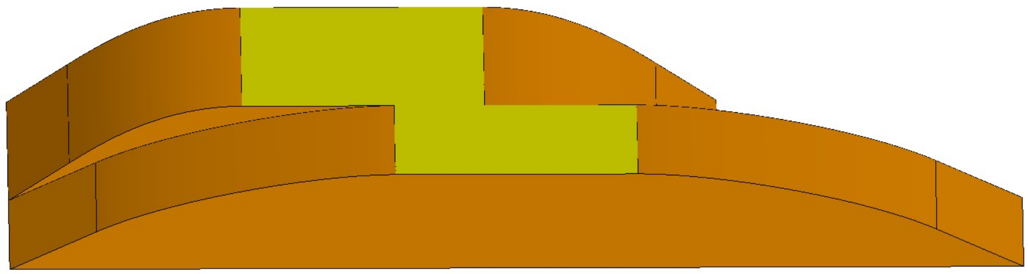

Figure 19: Bézier curves, D and d1 optimization model. This figure is a bottom-side view of both bézier curves. Both bézier curves had to optimized at the same time to get a common D and d1 values. The longer curve models that tip to tip bézier curves, while the shorter one models the side to side bézier curves.

Table 22: Bézier curves, D and d1 optimization values calculated by FEKO.

Inputs	**(ft)**
D	1.57
d1	0.84
bez_ang_side	1.17
bez_bot_side	2.14
bez_ang_pnt	2.23
bez_bot_pnt	2.18

6.3 Final Geometry Parameters

The final input geometry parameters for the antenna test fixture are listed in the Table 23. The the values of the bézier curves coordinates that created the curve are listed in Table 24. The other variables with the equations that were need to arrive at the final values are listed in Table 25.

Table 23: Final geometry input parameters for the antenna test fixture.

Inputs	**(Ft)**
Length (L)	12.50
Width (W)	8.75
Radius (R)	4.75
Height (H)	2.50
DUT edge (T)	3.50
Down size distance (D)	1.55
Down size height (d1)	0.84
Bez_Ang_pnt	2.23
Bez_Ang_side	1.17
Bez_Bot_pnt	2.18
Bez_Bot_side	1.75

Table 24: Final Bézier curve geometric values for the antenna test.

Bézier Curve Points	**x-axis (ft)**	**y-axis (ft)**	**z-axis (ft)**
Bez_point_pt_1	10.29	0	-0.84
Bez_point_pt_2	8.20	0	-1.63
Bez_point_pt_3	5.17	0	-2.50
Bez_point_pt_4	2.99	0	-2.50
Bez_side_pt_1	0	7.20	-0.84
Bez_side_pt_2	0	6.18	-1.39
Bez_side_pt_3	0	4.74	-2.50
Bez_side_pt_4	0	2.99	-2.50

Table 25: Final Variables with Equations for the antenna test fixture.

Varables	**Equations**
D_pnt	L-(L*scale1)
D_tang	sqrt(xt$^2 + yt^2) - sqrt((xt * scale1)^2 + (yt * scale1)^2$)
hyp_Bez_Ang_pnt	sqrt(D_pnt$^2 + d1^2) + Bez_Ang_pnt$
hyp_Bez_Ang_side	sqrt(D$^2 + d1^2) + Bez_Ang_side$
scale1	(W-D)/W
theta_Bez_pnt	arctan(d1/D_pnt)*180/pi
theta_Bez_side	arctan(d1/D)*180/pi
theta_L	arctan(yt/(L-xt))*180/pi
x_Bez_Ang_pnt	L-cos(theta_Bez_pnt*pi/180)*hyp_Bez_Ang_pnt
xt	(L*R$^2 + yo * R * sqrt(L^2 + yo^2 - R^2))/(L^2 + yo^2$)
y_Bez_Ang_side	W-cos(theta_Bez_side*pi/180)*hyp_Bez_Ang_side
yo	W-R
yt	sqrt(R$\hat{2}$-xt^2) + yo
z_Bez_Ang_pnt	-sin(theta_Bez_pnt*pi/180)*hyp_Bez_Ang_pnt
z_Bez_Ang_side	-sin(theta_Bez_side*pi/180)*hyp_Bez_Ang_side

6.4 Method of Moments (MoM) Setup

The Computational Electromagnetics (CEM) mothod that was used in FEKO for this effort was a subset of MoM called the Multilevel Fast Multipole Method (MLFMM). MLFMM is used for high mesh count constructs under certain geometry constraints. MLFMM collapses groups of mesh points that are far away from the current calculated point and sums it up to a single point for the calculations. Data storage precision was set to single precision, as the expected RCS values do not merit double precision. The field calculation methods for the Near-field and Far-field was set to Fast MLFMM based calculation, which is the default setting.

6.4.1 Mesh Requirements

Mesh size is a balance between computational power and the fidelity of the data and time limitations. Even with MLFMM the size and frequency requirements of this work produced long run-times. Feko offers only pre-select able mesh setting: fine, standard and course. The fine mesh setting is 16 points per wavelength, the standard mesh is 12 points per wavelength and course mesh is 8 points per wavelength. At 2000MHz with a standard mesh yielding 700K mesh count a full data run was estimated to take 25 days.

However, the design the of the test fixture has few edges and the rest is flat or smoothly varying, so a progressive mesh from the edges can significantly reduce the overall mesh count as shown in Figure 20. The edge is 16 point per wavelength with a radius of .16 wavelength (3 rows). Then, the middle is 10 point per wavelength with a radius of .437 wavelength (3 rows). Next, the inner is 9.5 point per wavelength with a radius of .63 wavelength (2 rows). Finally the rest is 7 point per wavelength, as shown in Figure 21. The mesh size at the point is similarly tapered. The point mesh is 30 points per wavelength with a of 0.2 wavelength radius which have 6 rows of mesh, as shown in Figure 22.

With this variable mesh that is a ratio to the wavelength the edges have a fine mesh while the rest of the test fixture is modeled just below a course mesh level. This brought the 2000MHz mesh count 700K for a standard mesh down to 320K mesh count with the edges having a Fine mesh for better fidelity. Simulation time went from 25 days down to 2.5 days.

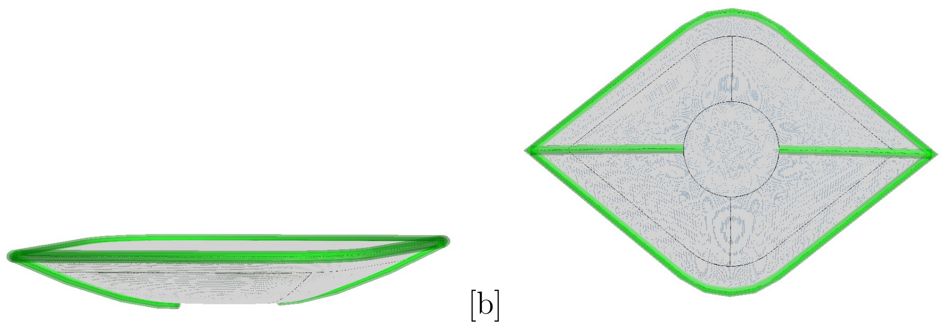

[a] [b]

Figure 20: Variable mesh size location on test fixture are in green (a) Side view (b) Bottom view

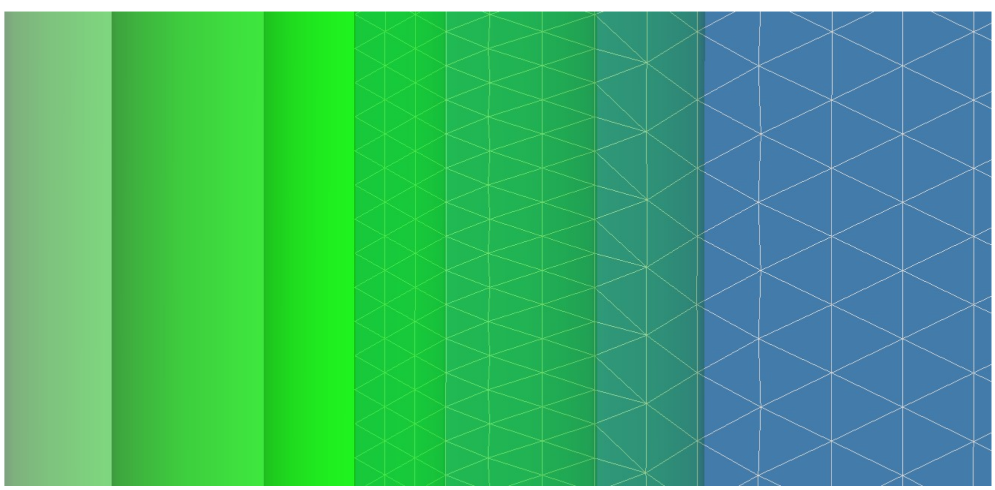

Figure 21: Variable mesh sizing from edge to smooth surface is a ratio to the wavelength. The edge is 16 point per wavelength with a radius of .16 wavelength (3 rows). Then, the middle is 10 point per wavelength with a radius of .437 wavelength (3 rows). Next, the inner is 9.5 point per wavelength with a radius of .63 wavelength (2 rows). finally the rest is 7 point per wavelength.

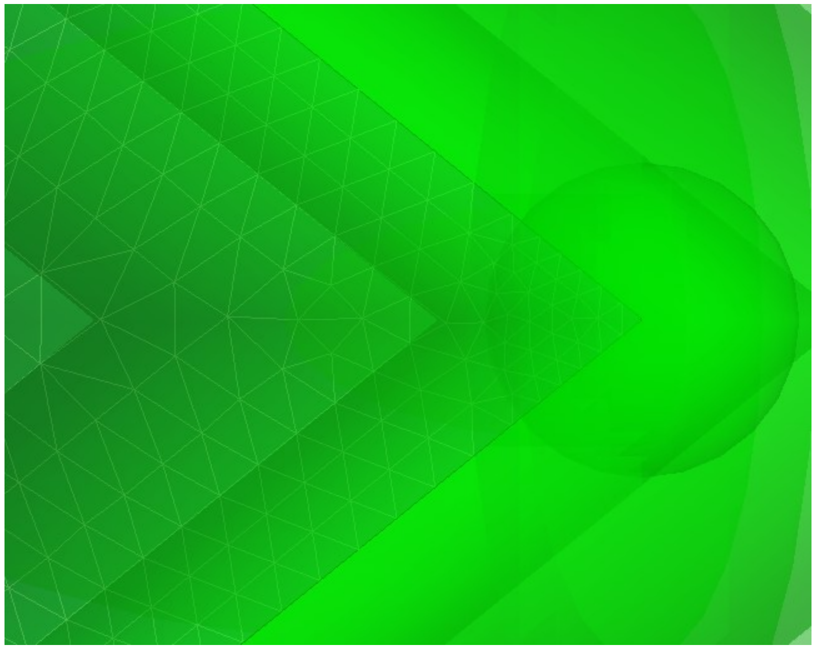

Figure 22: Mesh size at the point is a ratio to the wavelength. The point mesh is 30 points per wavelength with a of .2 wavelength radius which have 6 rows of mesh, which then flows into the variable mesh sizing from edge to smooth surface, as shown in Figure 21

6.4.2 Explanation of Geometry

Several geometric factors helped reduce the RCS signature of the test fixture. First, the aligned straight lines helped direct the spikes to desired location or direction. The second is the curve connecting the straight lines, which reduced tip scattering, in favor of mostly shadowed curve. The third is the limited width or the distance from the edge to the DUT, at the distance of five wavelengths. This allows enough distance for the nearfield to decay before getting to DUT, while minimizing nose-sector signature. Another perhaps under rated feature is the flat surface under the DUT and the same size as the DUT or large. This mitigates scatter due to a changing radius going from a curved surface to a flat surface in the near field. Last, lower test fixture profile design regions transition smoothly as second derivative continuous functions to reduce the RCS.

6.4.3 Anglular Resolution for RCS Calculations

The angular resolution for the final data productions azimuth values (phi) range from 0° to 45° degrees with increments of .1°. This was taken as a minimum for resolving spikes and nulls. For elevation (theta) the starting point is -5° and going to 40° with increments of 5°. As finer angular resolution in these cuts is generally not required.

6.5 RCS Data Production

Before beginning full production, a test of 3D model was conducted. This was done by running a simulation from Phi -60° to 60° and from -5° to 40° elevation (which is Theta 50° to 95° in spherical coordinates), Figure 23 shows the expected symmetry around Phi zero and the spike are in the correct location. The spike placement and symmetry suggest that so the 3-D model is a completely solid and with correct surface normals. Next, a spike walk test was conducted to ensure that they did not move into the Phi -45° to 45°region, as shown in Figure 24. With this information there is cause for reasonable confidence in the 0° to 45° results.

There were 9020 samples per frequency, so 72160 data point were created. The data was exported from PostFEKO and Air Force Institute of Technology (AFIT) Low Observables, Radar, and Electromagnetics (LORE) Processing Integrated Environment (ALPINE) was used to calculate the PCUM50 and PCUM90 data and generate plots.

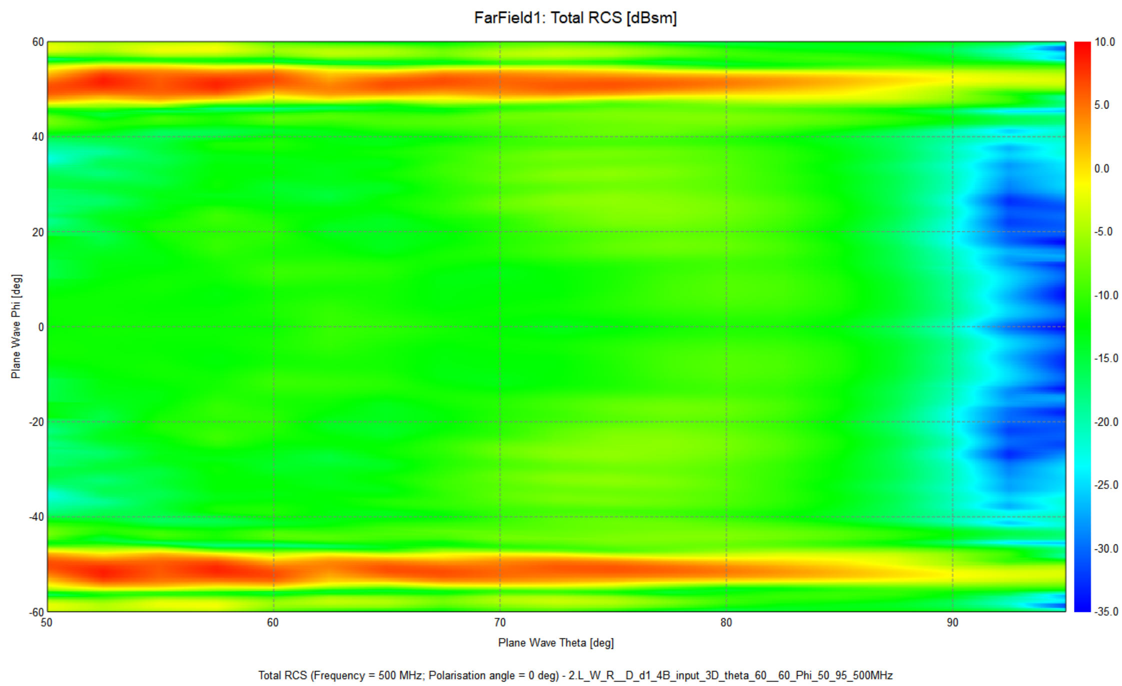

Figure 23: RCS surface plot at 500MHz, Phi -60° to -60° and elevation -5° to 40°. The dB range is -35 dB to 10 dB. This is to check if the 3-D object is correct by checking the splike locations and for symmetry around Phi 0.

6.5.1 Plots

The resulting 72160 data point would make 160 different plots, however on a set of exemplars are displayed. The data exported form PostFEKO and ALPINE was used to calculate the PCUM50 and PCUM90 data and generate plots. A consolidated RCS response surface plot RCS of the lower (Figure 25) and upper (Figure 26) frequency, shows the trend of the data. To demonstrate the RCS changes at the different frequencies the legend was set held constant for all of the surface plots with the lowest and highest values on the legend along the 8 plots, Figure 27.

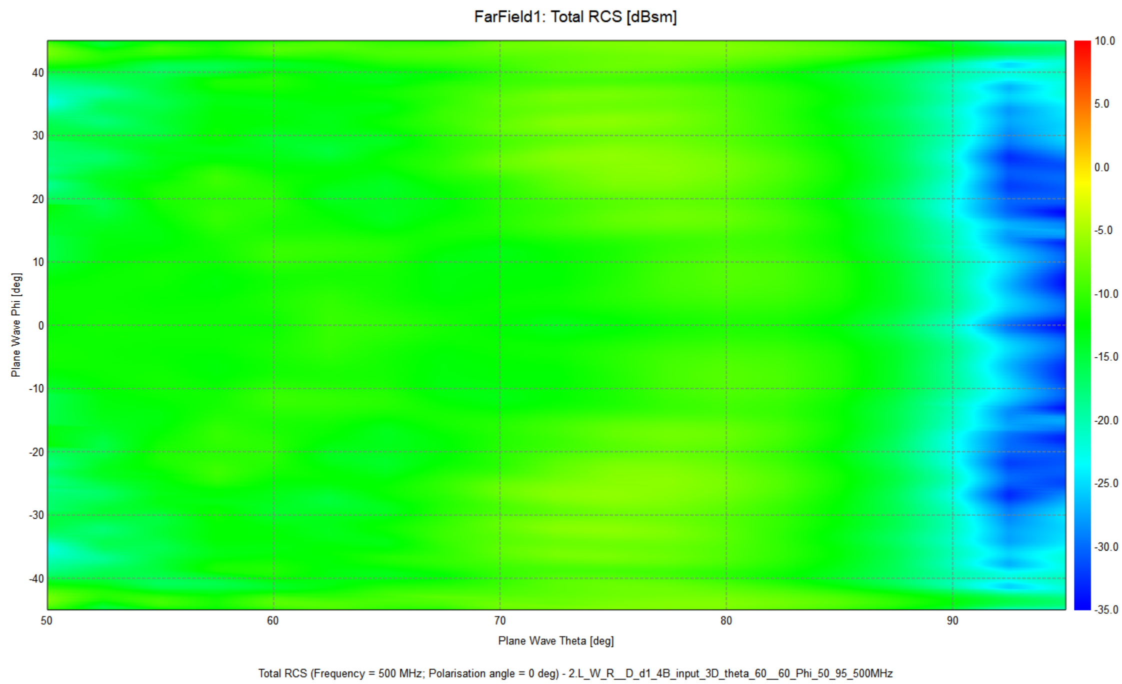

Figure 24: RCS surface plot at 500MHz, Phi -45° to -45° and elevation -5° to 40°. The dB range is -35 dB to 10 dB. This is to check if the spikes are in the test area are they are not.

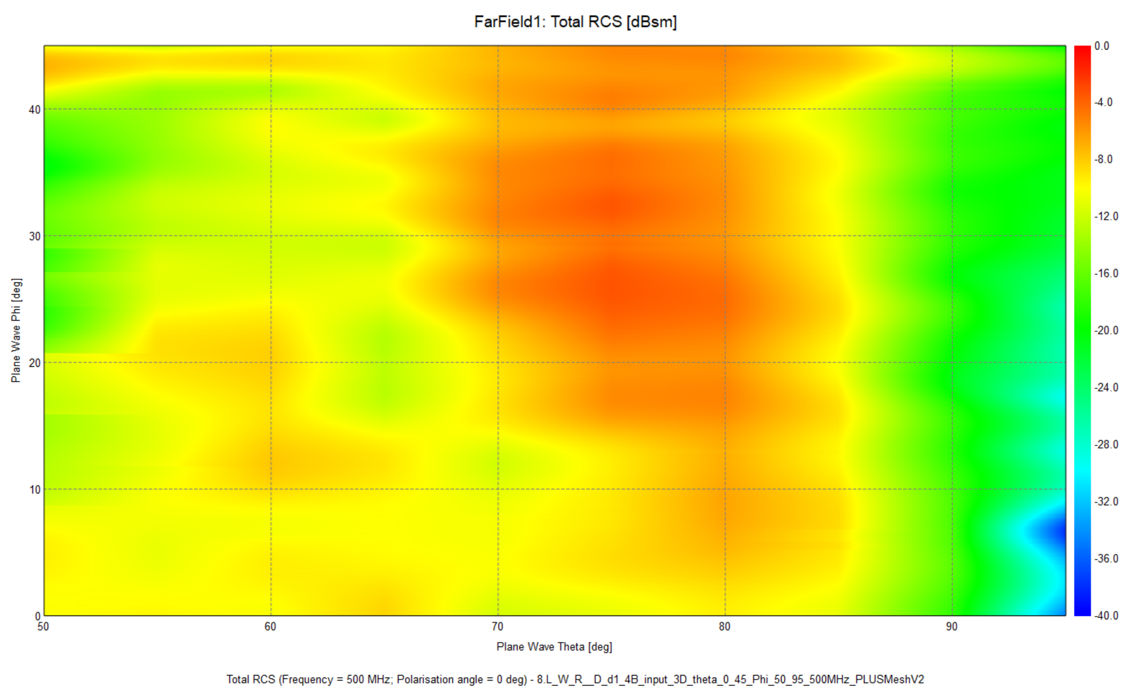

Figure 25: RCS surface plot at 500MHz, Phi 0° to 45° and elevation -5° to 40°. The dB range is -40 dB to 0 dB.

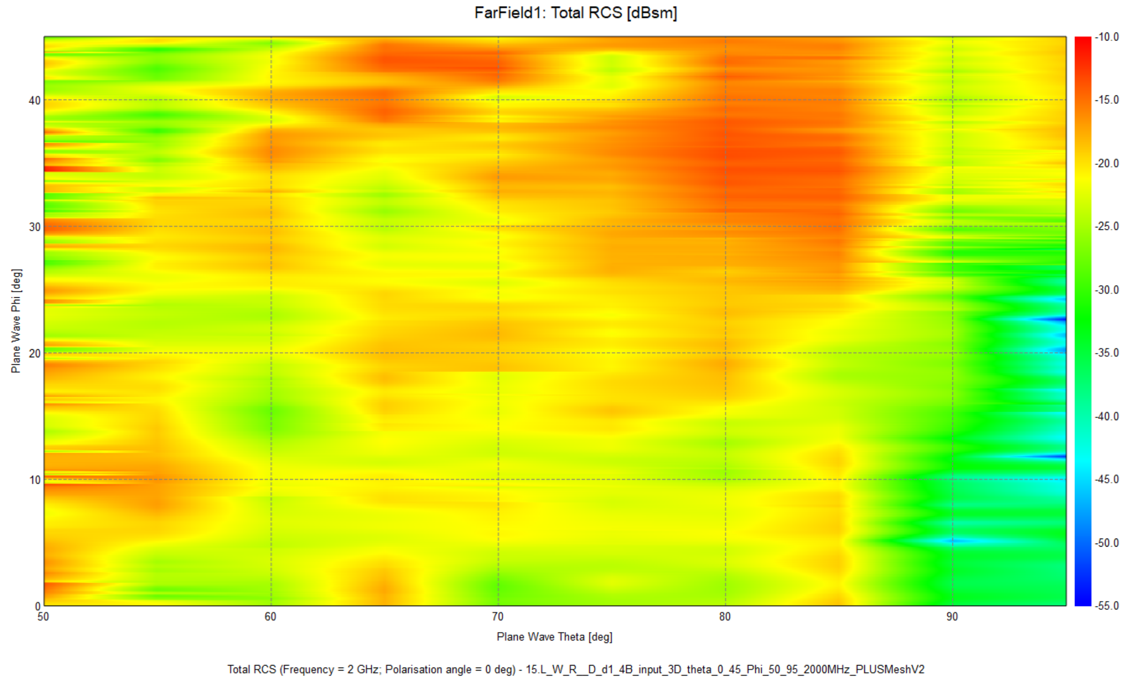

Figure 26: RCS surface plot at 2000MHz, Phi 0° to 45° and elevation -5° to 40°. The dB range is -55 dB to -10 dB.

As a bounding exercise , it was found that the PCUM50 PCUM90 Table 28 data and the RCS plots for 1550HMz cover the highs and lows on all four tables (PCUM50-tt, PCUM50-pp, PCUM90-tt and PCUM90-pp) across the different elevation which are -5° (Figure 28), 10° (Figure 29), 25° (Figure 30) and 40° (Figure 31). A detailed discussion is provided in Section 6.5.3.

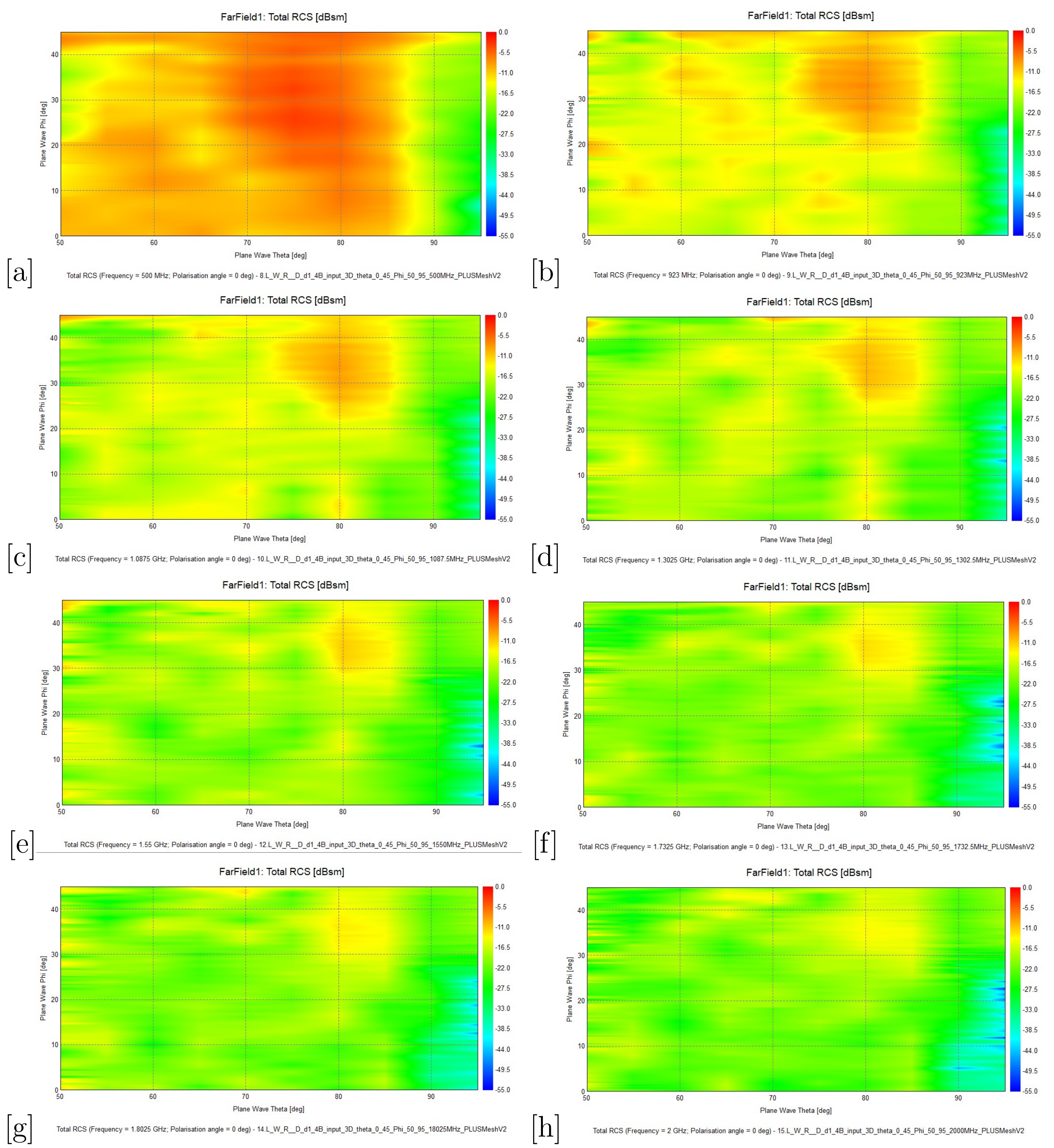

Figure 27: RCS surface plot of all frequencies. All figures range is -55 dB to 0 dB: (a) 500MHz (b) 923MHz (c) 1087.5MHz (d) 1302.5MHz (e) 1550MHz (f) 1732.5MHz (g) 1802.5MHz (h) 2000MHz. This shows how planform improves (low RCS) as frequency increase or as the electrical size increases.

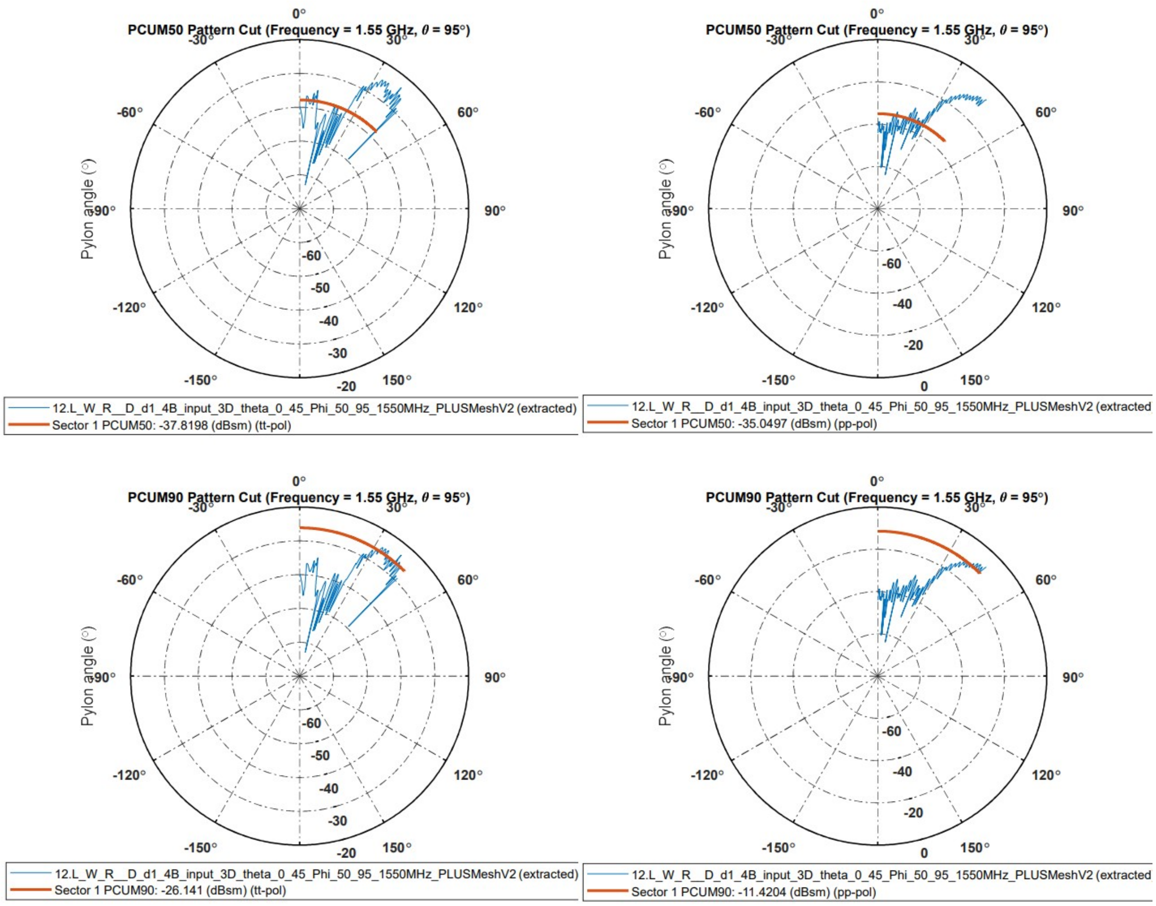

Figure 28: RCS plot at 1550MHz Phi 0° to 45°, and at -5° elevation. The tt plots on the right and pp plots on the left. PCUM50 on top and PCUM90 the bottom. For each of respective charts and with respect to 1550MHz frequency only. PCUM50-tt and PCUM50-pp is lowest RCS value for 1550MHz and PUCM50-tt is the 2nd lowest. PCUM90-pp is the hightest RCS, see Table 28.

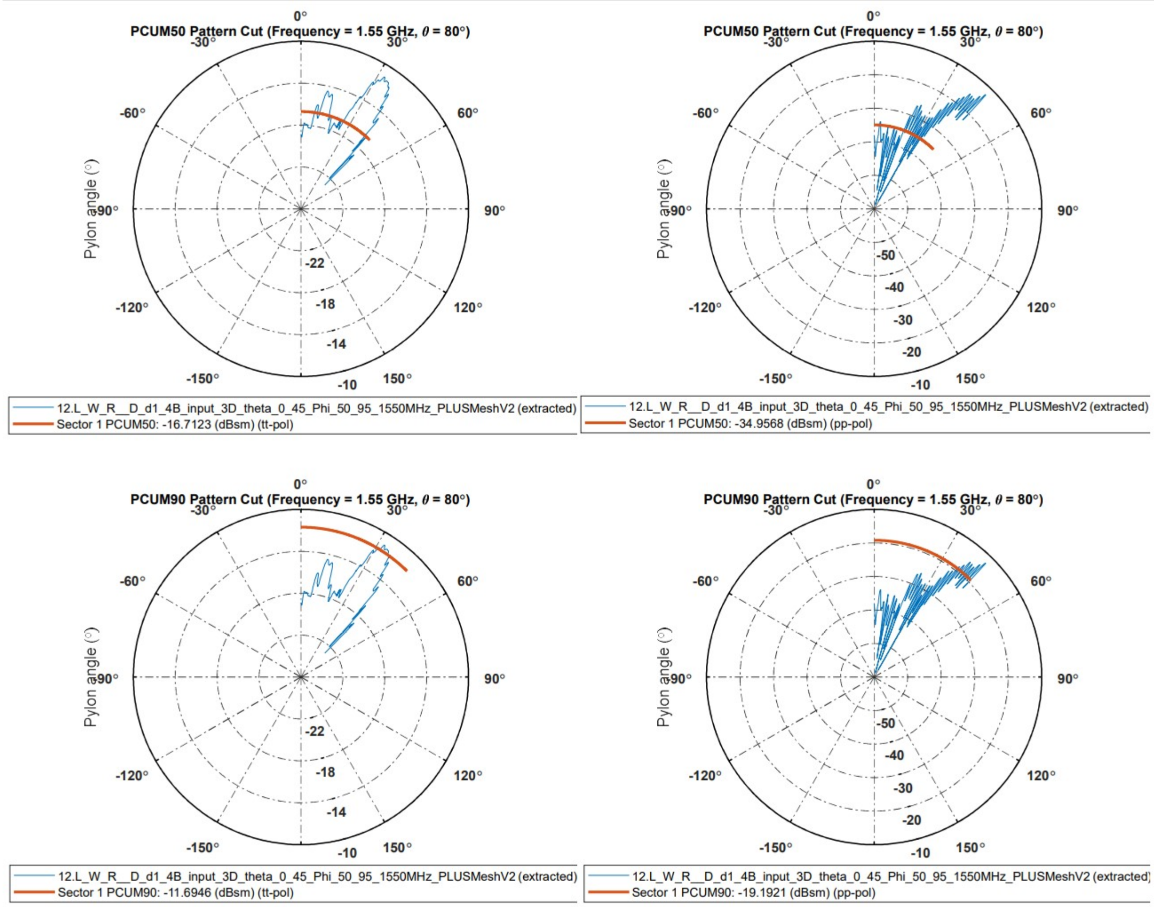

Figure 29: RCS plot at 1550MHz Phi 0° to 45°, and at 10° elevation. tt plots on the right and pp plots on the left. PCUM50 on top and PCUM90 the bottom. For each of respective charts and with respect to 1550MHz frequency only. PCUM50-tt and PCUM50-pp is highest RCS value for 1550MHz. PUCM50-tt and PCUM90-pp are middle RCS values, see Table 28.

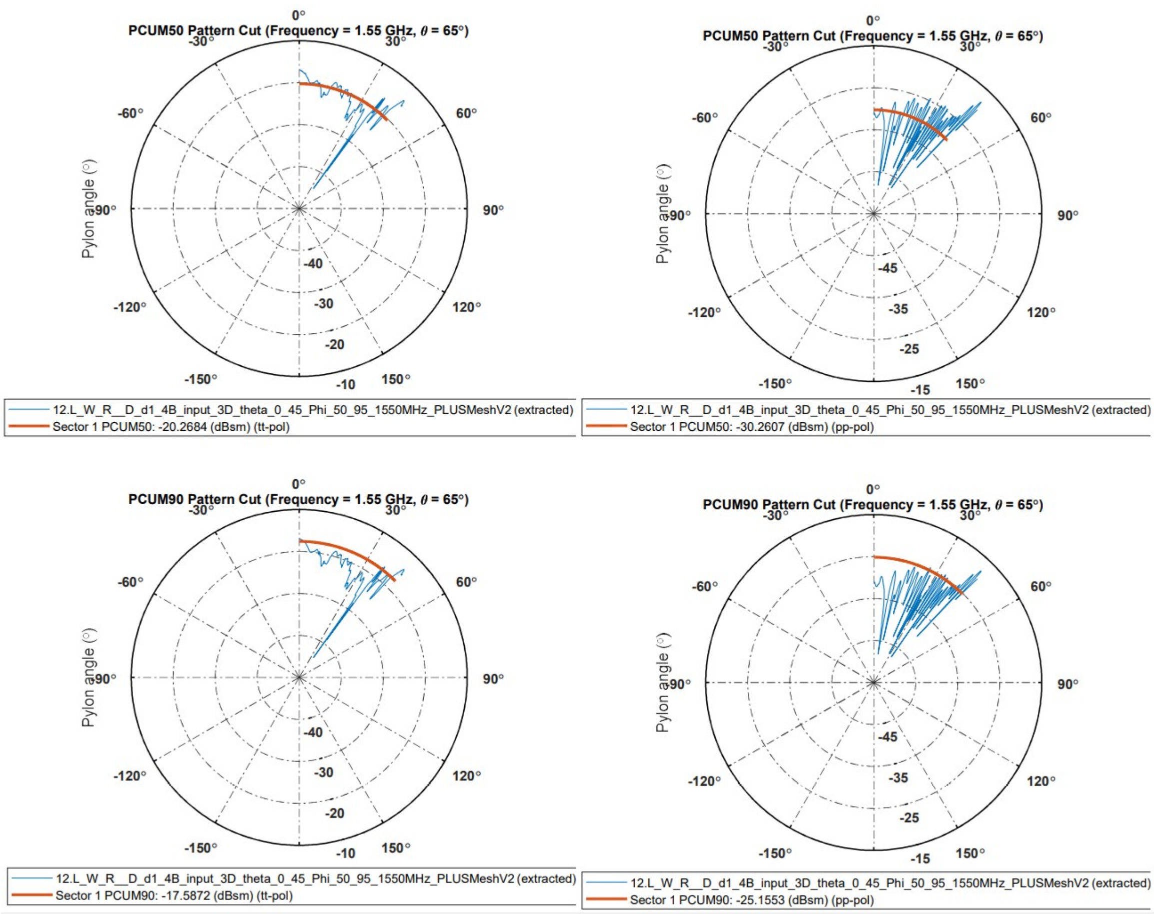

Figure 30: RCS plot at 1550MHz Phi 0° to 45°, and at 25° elevation. tt plots on the right and pp plots on the left. PCUM50 on top and PCUM90 the bottom. For each of respective charts and with respect to 1550MHz frequency only. PCUM90-pp is the lowest RCS value for 1550MHz. PUCM50-tt, PCUM90-tt and PCUM50-pp are middle RCS values, see Table 28.

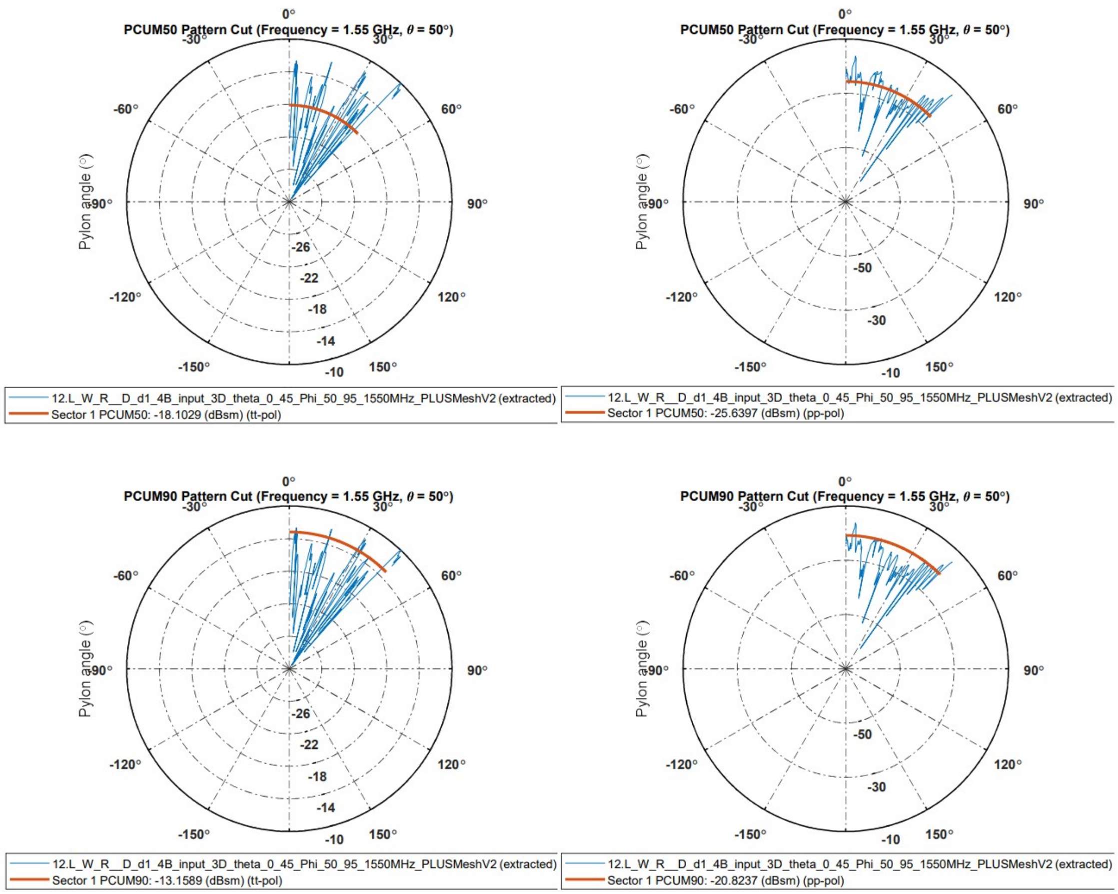

Figure 31: RCS plot at 1550MHz Phi 0° to 45°, and at 40° elevation. tt plots on the right and pp plots on the left. PCUM50 on top and PCUM90 the bottom. For each of respective charts and with respect to 1550MHz frequency only. PCUM50-pp is hightest RCS value for 1550MHz and PUCM50-tt and PCUM590-tt is the 2nd highest. PCUM90-pp is the middlet RCS value, see Table 28.

6.5.2 Angular PCUM50 and PCUM90 Data

The final data for PCUM50 and PCUM 90 for both the Vertical Polarization (tt) and Horizontal Polarization (pp) is shown in one table to be able to compare the different values of Table 26, Table 27 and Table 28. The data is the same for all three tables the only difference is the conditional formatting by color to highlight different patterns. Table 26 conditional formatting is by color for all the of the values. Table 27 conditional formatting is by color per chart, i.e. PCUM50-tt, PCUM50-pp. Table 28 conditional formatting by color is per frequency. i.e. PCUM50-tt at 500MHz, PCUM50-tt at 923.0MHz. These tables will be used in the section 6.5.3 for the final analysis.

Table 26: Final PCUM50 and PCUM90 for tt and pp in dB and which is from 0° to 45° with 0.1° steps for each elevation starting at -5° to 40° with 5° steps. Conditional Formatting for the color scale was for all data.

Vertical Polarzation (tt)

	Elev.	Frequency (MHz)							
		500.0	923.0	1087.5	1302.5	1550.0	1732.5	1802.5	2000.0
PCUM50	40	-15.11	-15.97	-21.03	-20.92	-18.10	-20.47	-19.22	-22.42
	35	-11.60	-16.13	-17.69	-18.71	-19.55	-22.60	-21.23	-23.59
	30	-10.34	-15.66	-18.76	-21.29	-21.41	-22.80	-23.31	-23.47
	25	-12.76	-14.79	-16.40	-17.70	-20.27	-22.00	-20.95	-20.74
	20	-10.24	-16.83	-16.16	-17.80	-18.89	-20.99	-21.50	-22.43
	15	-8.01	-14.01	-17.03	-20.79	-20.34	-21.57	-21.33	-21.35
	10	-7.06	-13.66	-13.55	-14.07	-16.71	-17.87	-17.84	-19.06
	5	-10.92	-16.16	-16.87	-18.77	-20.82	-19.97	-19.64	-19.88
	0	-22.11	-23.02	-23.83	-24.55	-27.64	-31.14	-32.48	-33.43
	-5	-33.78	-38.37	-37.76	-38.20	-37.82	-36.88	-36.69	-37.42
PCUM90	Elev.	Frequency (MHz)							
		500.0	923.0	1087.5	1302.5	1550.0	1732.5	1802.5	2000.0
	40	-9.69	-11.66	-16.07	-15.42	-13.16	-15.26	-14.05	-16.95
	35	-9.89	-13.19	-14.90	-15.53	-16.67	-17.97	-17.46	-19.32
	30	-8.73	-13.81	-15.27	-17.77	-18.14	-19.06	-19.55	-20.08
	25	-9.40	-12.73	-15.00	-15.28	-17.59	-18.72	-18.66	-17.38
	20	-6.04	-13.34	-13.96	-14.64	-16.24	-17.60	-17.07	-18.65
	15	-4.12	-10.20	-12.40	-15.39	-17.86	-18.44	-18.74	-18.13
	10	-5.43	-8.42	-9.27	-10.45	-11.69	-12.74	-13.53	-14.65
	5	-9.13	-13.19	-13.96	-14.37	-15.11	-15.30	-15.35	-15.72
	0	-17.23	-19.17	-20.84	-23.40	-25.12	-25.62	-25.71	-26.73
	-5	-27.61	-27.19	-27.18	-26.79	-26.14	-25.71	-25.52	-25.18

5.Horizontal Polarzation (pp)

	Elev.	Frequency (MHz)							
		500.0	923.0	1087.5	1302.5	1550.0	1732.5	1802.5	2000.0
PCUM50	40	-18.55	-23.46	-24.08	-24.55	-25.64	-27.42	-26.34	-27.10
	35	-20.44	-23.03	-24.42	-25.75	-27.75	-28.86	-27.22	-29.36
	30	-20.53	-28.50	-29.25	-29.69	-31.51	-33.69	-34.27	-33.07
	25	-22.02	-28.90	-29.02	-29.73	-30.26	-32.13	-33.20	-34.74
	20	-24.23	-27.21	-28.44	-31.03	-31.37	-32.80	-33.63	-34.83
	15	-23.85	-29.81	-31.07	-32.15	-33.75	-34.35	-35.25	-36.76
	10	-20.34	-29.75	-31.17	-34.30	-34.96	-36.51	-35.76	-37.76
	5	-16.92	-29.18	-31.35	-34.22	-36.11	-37.61	-35.02	-37.50
	0	-16.02	-29.28	-30.75	-33.04	-34.45	-36.40	-36.59	-38.17
	-5	-17.30	-28.99	-31.46	-32.42	-35.05	-36.25	-36.81	-37.52
PCUM90	Elev.	Frequency (MHz)							
		500.0	923.0	1087.5	1302.5	1550.0	1732.5	1802.5	2000.0
	40	-14.57	-18.83	-19.61	-18.53	-20.82	-22.02	-19.58	-20.71
	35	-14.41	-18.77	-20.44	-20.23	-22.22	-24.88	-20.50	-25.76
	30	-15.39	-19.22	-21.03	-25.23	-24.23	-26.30	-26.53	-26.46
	25	-15.49	-20.39	-22.15	-23.15	-25.16	-26.04	-25.69	-28.89
	20	-13.31	-20.18	-20.61	-21.68	-24.23	-25.83	-25.97	-26.30
	15	-11.63	-19.35	-21.43	-23.47	-23.14	-22.90	-23.30	-23.32
	10	-8.73	-13.16	-14.96	-16.28	-19.19	-20.56	-20.97	-22.41
	5	-6.47	-10.13	-11.19	-12.51	-13.62	-14.43	-14.57	-15.64
	0	-5.53	-8.81	-9.73	-10.91	-11.62	-12.12	-12.38	-13.08
	-5	-5.33	-8.46	-9.40	-10.43	-11.42	-12.00	-12.19	-12.91

Table 27: Final PCUM50 and PCUM90 for tt and pp in dB and which is from 0° to 45° with 0.1° steps for each elevation starting at -5° to 40° with 5° steps. Conditional Formatting for the color scale was per chart. i.e. PCUM50-tt, PCUM50-pp.

PCUM50 — Vertical Polarzation (tt)

Elev.	Frequency (MHz) 500.0	923.0	1087.5	1302.5	1550.0	1732.5	1802.5	2000.0
40	-15.11	-15.97	-21.03	-20.92	-18.10	-20.47	-19.22	-22.42
35	-11.60	-16.13	-17.69	-18.71	-19.55	-22.60	-21.23	-23.59
30	-10.34	-15.66	-18.76	-21.29	-21.41	-22.80	-23.31	-23.47
25	-12.76	-14.79	-16.40	-17.70	-20.27	-22.00	-20.95	-20.74
20	-10.24	-16.83	-16.16	-17.80	-18.89	-20.99	-21.50	-22.43
15	-8.01	-14.01	-17.03	-20.79	-20.34	-21.57	-21.33	-21.35
10	-7.06	-13.66	-13.55	-14.07	-16.71	-17.87	-17.84	-19.06
5	-10.92	-16.16	-16.87	-18.77	-20.82	-19.97	-19.64	-19.88
0	-22.11	-23.02	-23.83	-24.55	-27.64	-31.14	-32.48	-33.43
-5	-33.78	-38.37	-37.76	-38.20	-37.82	-36.88	-36.69	-37.42

PCUM50 — 5.Horizontal Polarzation (pp)

Elev.	Frequency (MHz) 500.0	923.0	1087.5	1302.5	1550.0	1732.5	1802.5	2000.0
40	-18.55	-23.46	-24.08	-24.55	-25.64	-27.42	-26.34	-27.10
35	-20.44	-23.03	-24.42	-25.75	-27.75	-28.86	-27.22	-29.36
30	-20.53	-28.50	-29.25	-29.69	-31.51	-33.69	-34.27	-33.07
25	-22.02	-28.90	-29.02	-29.73	-30.26	-32.13	-33.20	-34.74
20	-24.23	-27.21	-28.44	-31.03	-31.37	-32.80	-33.63	-34.83
15	-23.85	-29.81	-31.07	-32.15	-33.75	-34.35	-35.25	-36.76
10	-20.34	-29.75	-31.17	-34.30	-34.96	-36.51	-35.76	-37.76
5	-16.92	-29.18	-31.35	-34.22	-36.11	-37.61	-35.02	-37.50
0	-16.02	-29.28	-30.75	-33.04	-34.45	-36.40	-36.59	-38.17
-5	-17.30	-28.99	-31.46	-32.42	-35.05	-36.25	-36.81	-37.52

PCUM90 — Vertical Polarzation (tt)

Elev.	Frequency (MHz) 500.0	923.0	1087.5	1302.5	1550.0	1732.5	1802.5	2000.0
40	-9.69	-11.66	-16.07	-15.42	-13.16	-15.26	-14.05	-16.95
35	-9.89	-13.19	-14.90	-15.53	-16.67	-17.97	-17.46	-19.32
30	-8.73	-13.81	-15.27	-17.77	-18.14	-19.06	-19.55	-20.08
25	-9.40	-12.73	-15.00	-15.28	-17.59	-18.72	-18.66	-17.38
20	-6.04	-13.34	-13.96	-14.64	-16.24	-17.60	-17.07	-18.65
15	-4.12	-10.20	-12.40	-15.39	-17.86	-18.44	-18.74	-18.13
10	-5.43	-8.42	-9.27	-10.45	-11.69	-12.74	-13.53	-14.65
5	-9.13	-13.19	-13.96	-14.37	-15.11	-15.30	-15.35	-15.72
0	-17.23	-19.17	-20.84	-23.40	-25.12	-25.62	-25.71	-26.73
-5	-27.61	-27.19	-27.18	-26.79	-26.14	-25.71	-25.52	-25.18

PCUM90 — 5.Horizontal Polarzation (pp)

Elev.	Frequency (MHz) 500.0	923.0	1087.5	1302.5	1550.0	1732.5	1802.5	2000.0
40	-14.57	-18.83	-19.61	-18.53	-20.82	-22.02	-19.58	-20.71
35	-14.41	-18.77	-20.44	-20.23	-22.22	-24.88	-20.50	-25.76
30	-15.39	-19.22	-21.03	-25.23	-24.23	-26.30	-26.53	-26.46
25	-15.49	-20.39	-22.15	-23.15	-25.16	-26.04	-25.69	-28.89
20	-13.31	-20.18	-20.61	-21.68	-24.23	-25.83	-25.97	-26.30
15	-11.63	-19.35	-21.43	-23.47	-23.14	-22.90	-23.30	-23.32
10	-8.73	-13.16	-14.96	-16.28	-19.19	-20.56	-20.97	-22.41
5	-6.47	-10.13	-11.19	-12.51	-13.62	-14.43	-14.57	-15.64
0	-5.53	-8.81	-9.73	-10.91	-11.62	-12.12	-12.38	-13.08
-5	-5.33	-8.46	-9.40	-10.43	-11.42	-12.00	-12.19	-12.91

6.5.3 Analysis

No specific RCS goal was given for this effort. The objective was to make this RCS as low as possible, within constraints. The general trend of the results are as follows. First, as the frequency increased the RCS becomes smaller, as shown in Figure 27. Second, the pp-polarized values were lower than the tt-polarized values, this is due to the pp orientation having a greater surface area parallel to it than the tt case, as is typical for this type of structure and shown in Table 26.

For the tt PCUM 50 and PCUM90 null and peak locations are similar, as shown in Table 27. The lowest and highest RCS are close to each other. This is due to the back edge diffraction which is block by the test fixture at -5°. However at 10° elevation the highest value of RCS is observed because there is more efficient surface wave coupling and there is direct illumination of the edge trailing edge, as shown in table 28 and Figure 31.

Table 28: Final PCUM50 and PCUM90 for tt and pp in dB and which is from 0° to 45° with 0.1° steps for each elevation starting at -5° to 40° with 5° steps. Conditional Formatting for the color scale was per frequency. i.e. PCUM50-tt at 500MHz, PCUM50-tt at 923.0MHz.

PCUM50 — Vertical Polarzation (tt)

Elev.	Frequency (MHz)							
	500.0	923.0	1087.5	1302.5	1550.0	1732.5	1802.5	2000.0
40	-15.11	-15.97	-21.03	-20.92	-18.10	-20.47	-19.22	-22.42
35	-11.60	-16.13	-17.69	-18.71	-19.55	-22.60	-21.23	-23.59
30	-10.34	-15.66	-18.76	-21.29	-21.41	-22.80	-23.31	-23.47
25	-12.76	-14.79	-16.40	-17.70	-20.27	-22.00	-20.95	-20.74
20	-10.24	-16.83	-16.16	-17.80	-18.89	-20.99	-21.50	-22.43
15	-8.01	-14.01	-17.03	-20.79	-20.34	-21.57	-21.33	-21.35
10	-7.06	-13.66	-13.55	-14.07	-16.71	-17.87	-17.84	-19.06
5	-10.92	-16.16	-16.87	-18.77	-20.82	-19.97	-19.64	-19.88
0	-22.11	-23.02	-23.83	-24.55	-27.64	-31.14	-32.48	-33.43
-5	-33.78	-38.37	-37.76	-38.20	-37.82	-36.88	-36.69	-37.42

PCUM50 — 5.Horizontal Polarzation (pp)

Elev.	Frequency (MHz)							
	500.0	923.0	1087.5	1302.5	1550.0	1732.5	1802.5	2000.0
40	-18.55	-23.46	-24.08	-24.55	-25.64	-27.42	-26.34	-27.10
35	-20.44	-23.03	-24.42	-25.75	-27.75	-28.86	-27.22	-29.36
30	-20.53	-28.50	-29.25	-29.69	-31.51	-33.69	-34.27	-33.07
25	-22.02	-28.90	-29.02	-29.73	-30.26	-32.13	-33.20	-34.74
20	-24.23	-27.21	-28.44	-31.03	-31.37	-32.80	-33.63	-34.83
15	-23.85	-29.81	-31.07	-32.15	-33.75	-34.35	-35.25	-36.76
10	-20.34	-29.75	-31.17	-34.30	-34.96	-36.51	-35.76	-37.76
5	-16.92	-29.18	-31.35	-34.22	-36.11	-37.61	-35.02	-37.50
0	-16.02	-29.28	-30.75	-33.04	-34.45	-36.40	-36.59	-38.17
-5	-17.30	-28.99	-31.46	-32.42	-35.05	-36.25	-36.81	-37.52

PCUM90 — Vertical Polarzation (tt)

Elev.	Frequency (MHz)							
	500.0	923.0	1087.5	1302.5	1550.0	1732.5	1802.5	2000.0
40	-9.69	-11.66	-16.07	-15.42	-13.16	-15.26	-14.05	-16.95
35	-9.89	-13.19	-14.90	-15.53	-16.67	-17.97	-17.46	-19.32
30	-8.73	-13.81	-15.27	-17.77	-18.14	-19.06	-19.55	-20.08
25	-9.40	-12.73	-15.00	-15.28	-17.59	-18.72	-18.66	-17.38
20	-6.04	-13.34	-13.96	-14.64	-16.24	-17.60	-17.07	-18.65
15	-4.12	-10.20	-12.40	-15.39	-17.86	-18.44	-18.74	-18.13
10	-5.43	-8.42	-9.27	-10.45	-11.69	-12.74	-13.53	-14.65
5	-9.13	-13.19	-13.96	-14.37	-15.11	-15.30	-15.35	-15.72
0	-17.23	-19.17	-20.84	-23.40	-25.12	-25.62	-25.71	-26.73
-5	-27.61	-27.19	-27.18	-26.79	-26.14	-25.71	-25.52	-25.18

PCUM90 — 5.Horizontal Polarzation (pp)

Elev.	Frequency (MHz)							
	500.0	923.0	1087.5	1302.5	1550.0	1732.5	1802.5	2000.0
40	-14.57	-18.83	-19.61	-18.53	-20.82	-22.02	-19.58	-20.71
35	-14.41	-18.77	-20.44	-20.23	-22.22	-24.88	-20.50	-25.76
30	-15.39	-19.22	-21.03	-25.23	-24.23	-26.30	-26.53	-26.46
25	-15.49	-20.39	-22.15	-23.15	-25.16	-26.04	-25.69	-28.89
20	-13.31	-20.18	-20.61	-21.68	-24.23	-25.83	-25.97	-26.30
15	-11.63	-19.35	-21.43	-23.47	-23.14	-22.90	-23.30	-23.32
10	-8.73	-13.16	-14.96	-16.28	-19.19	-20.56	-20.97	-22.41
5	-6.47	-10.13	-11.19	-12.51	-13.62	-14.43	-14.57	-15.64
0	-5.53	-8.81	-9.73	-10.91	-11.62	-12.12	-12.38	-13.08
-5	-5.33	-8.46	-9.40	-10.43	-11.42	-12.00	-12.19	-12.91

For the pp PCUM50 and PCUM90 there are very few similarities. Where the PCUM50 has a very low RCS the PCUM90 has very high RCS, as shown in Table 28. This is due to the low RCS until there is a spike near the 45° point, or efficient planform behavior. There the diffractive contribution from the long edge of the test fixture, parallel to the pp-polarized field, results in strong currents, the results of which appear in Figure 28. However, with the increase of elevation the pp-polarized field less efficiently excited currents and the signature is reduced.

VII. Conclusions

A viable uncoated antenna Radar Cross-Section (RCS) test fixture design was developed subject to a great many constraints. First, the constraints were evaluated, and some required adjustments were made. Second, a study of the upper profile geometry for planform was conducted and the profiles down-selected to the radius/straight design. Next, to select the proper size, a limited response surface in geometry and RCS was developed. This data was used to conduct a trade space analysis on RCS versus the Device Under Test (DUT) standoff distance, driving the final size selected. Finally, a full geometry and RCS data set was developed, produced, and analyzed as part of the modeling data package for the sponsor.

7.1 Future Work

The following future work is recommended.

- Validate simulations by creating a subscale physical model and compare the simulation to the model's results.
- Investigation specular and non-specular Radar Absorbing Material (RAM) to further reduce the RCS signature.
- Additional refinement on the design based on how the test fixture will be deployed within the radar range.

Bibliography

1. Robert O'Donnell. Introduction to Radar Systems, 2018.

2. Rebecca (A Mitchell Institute Study) Grant. *The Radar Game Understanding Stealth and Aircraft Survivability.* Mitchell Institute Press, Arlington, VA, 2010.

3. Jr. Lynch, David. *Introduction to RF Stealth.* SciTech Publishing Inc., Raleigh, 1 edition, 2004.

4. Constantine A. Ballanis. *Antenna Theory Analysis and Design.* John Wiley Sons, Inc., Hoboken, NJ, 3rd edition, 2005.

5. William A. Richares, Mark A.; Scheer, James A.; Holm. *Principles of Modern Radar Volume I - Basic Principles.* SciTech Publishing, Inc, Raleigh, NC, 2010.

6. W. Wiesbeck and E. Heidrich. Influence of antennas on the radar cross section of camouflaged aircraft. In *92 International Conference on Radar*, pages 122–125, 1992.

7. Jie Xu, Meie Chen, and Junhong Wang. Low rcs microstrip antenna with uniplanar compact electromagnetic bandgap substrate. In *2013 IEEE INTERNATIONAL CONFERENCE ON MICROWAVE TECHNOLOGY COMPUTATIONAL ELECTROMAGNETICS*, pages 308–311, 2013.

8. Hong-Kyu Jang, Jae-Hwan Shin, and Chun-Gon Kim. Low rcs patch array antenna with electromagnetic bandgap using a conducting polymer. In *2010 International Conference on Electromagnetics in Advanced Applications*, pages 140–143, 2010.

9. J.A.G. McNamara, D.A.; Pistorius C.W.I. ; Malherve. *Introduction to the Uniform Geometrical Theory of Diffraction*. ARTECH HOUSE, Norwood, MA, 2nd edition, 1990.

10. Shiquan Hao, Yajun Liu, Feng Xu, Jingran Yuan, and Wenhao Liu. Research on the shape stealth design of infantry fighting vehicle. In *2021 6th International Conference on Intelligent Computing and Signal Processing (ICSP)*, pages 1393–1396, 2021.

11. Mauro A. Alves, Rafael J. Port, and Mirabel C. Rezende. Simulations of the radar cross section of a stealth aircraft. In *2007 SBMO/IEEE MTT-S International Microwave and Optoelectronics Conference*, pages 409–412, 2007.

12. Department of Defense. Strategic Spectrum Plan Submitted to the Department of Commerce. *Training*, (February):108, 2008.

13. DOD 2020. Department of Defense Electromagnetic Spectrum Superiority Strategy. Technical report, 2020.

14. 2021 FCC. FCC ALLOCATION HISTORY FILE. Technical report, 2021.

Acronyms

3-D Three Dimensions. vii, 55, 56, 63, 64

AFIT Air Force Institute of Technology. 14, 63, 79

ALPINE Air Force Institute of Technology (AFIT) Low Observables, Radar, and Electromagnetics (LORE) Processing Integrated Environment. 14, 63, 64

CAD Computer-Aided Design. 56

CEM Computational Electromagnetics. v, 6, 8, 29, 60

DoD Department of Defense. ix, 41, 42, 54

DUT Device Under Test. vi, ix, 3, 4, 9, 10, 11, 12, 18, 19, 22, 24, 29, 34, 40, 41, 43, 48, 49, 50, 51, 54, 55, 62, 76

FCC Federal Communications Commission. 41

GO Geometric Optics. 6, 8, 12, 13, 14, 17, 29

GTD Geometrical Theory of Diffraction. 6, 8

LO Low Observable. 1

LORE Low Observables, Radar, and Electromagnetics. 14, 63, 79

MLFMM Multilevel Fast Multipole Method. 29, 60

MoM Method of Moments. vi, 6, 7, 8, 9, 29, 40, 60

PEC perfect electric conductor. vii, 8, 13

RAM Radar Absorbing Material. 9, 76

RCS Radar Cross-Section. iv, v, vi, vii, viii, ix, x, 1, 2, 6, 7, 8, 9, 10, 12, 13, 14, 17, 27, 28, 29, 31, 32, 33, 34, 38, 41, 42, 44, 46, 47, 51, 52, 53, 54, 55, 60, 62, 63, 64, 65, 66, 67, 68, 69, 70, 71, 73, 75, 76, 1

tt-pol theta-theta polarization. 31

UTD Uniform Theory of Diffraction. 8

REPORT DOCUMENTATION PAGE

Form Approved
OMB No. 0704–0188

1. REPORT DATE (DD–MM–YYYY)	2. REPORT TYPE	3. DATES COVERED (From — To)
24–03–2020	Master's Thesis	Sept 2020 — Mar 2022

4. TITLE AND SUBTITLE

Design Study for an Antenna Radar Cross Section Measurement Test Fixture

5a. CONTRACT NUMBER

5b. GRANT NUMBER

5c. PROGRAM ELEMENT NUMBER

6. AUTHOR(S)

Kreimeyer, Wayne C, Capt, USAF

5d. PROJECT NUMBER

5e. TASK NUMBER

5f. WORK UNIT NUMBER

7. PERFORMING ORGANIZATION NAME(S) AND ADDRESS(ES)

Air Force Institute of Technology
Graduate School of Engineering and Management (AFIT/EN)
2950 Hobson Way
WPAFB OH 45433-7765

8. PERFORMING ORGANIZATION REPORT NUMBER

AFIT-ENG-MS-22-M-040

9. SPONSORING / MONITORING AGENCY NAME(S) AND ADDRESS(ES)

Intentionally Left Blank

10. SPONSOR/MONITOR'S ACRONYM(S)

11. SPONSOR/MONITOR'S REPORT NUMBER(S)

12. DISTRIBUTION / AVAILABILITY STATEMENT

DISTRIBUTION STATEMENT A:
APPROVED FOR PUBLIC RELEASE; DISTRIBUTION UNLIMITED.

13. SUPPLEMENTARY NOTES

14. ABSTRACT

Stealth aircraft are designed to be undetected by radar by minimizing a return signature called the Radar Cross Section, (RCS). Therefore, it is essential to understand how antennas, which are necessary for communication, affect the overall RCS of the aircraft, so that their effects can be managed. Antenna RCS is commonly measured in a compact range, at a component level. So, the antenna needs a structure to support it, also referred to as a test fixture, that does not interfere with the measurement process. This thesis seeks to minimize the RCS of a test fixture, over a particular frequency band, while meeting other geometric constraints by evaluating different geometries. The result of this thesis is a test fixture design that has a low RCS which is separable from the signature of the antenna under measurement, while providing an appropriate near field environment for the antenna.

15. SUBJECT TERMS

Radar Cross Section, RCS, Test Fixture, Mesh, Geometric Optics, GO, Antenna, Low Observable, LO, Stealth, Device Under Test, DUT, Geometrical Theory of Diffraction, GTD, Method of Moments, MoM, Multilevel Fast Multipole Method, MLFMM

16. SECURITY CLASSIFICATION OF:			17. LIMITATION OF ABSTRACT	18. NUMBER OF PAGES	19a. NAME OF RESPONSIBLE PERSON
a. REPORT	b. ABSTRACT	c. THIS PAGE			Lt Col Michael D. Seal, AFIT/ENG
					19b. TELEPHONE NUMBER (include area code)
U	U	U	UU	92	(937)255-3636 x3305 michael.seal@afit.edu